Strong interaction matter in the universe

Achim Schwenk
TECHNISCHE UNIVERSITÄT DARMSTADT
EMMI
MAX-PLANCK-INSTITUT FÜR KERNPHYSIK HEIDELBERG

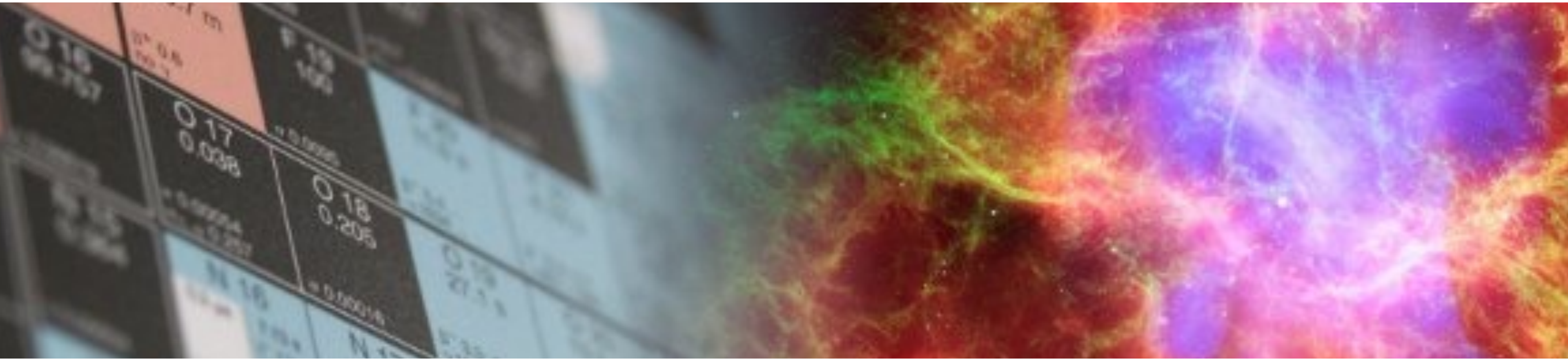

10 Years MITP, Mainz, May 9, 2023

DFG
SFB 1245
erc
European Research Council
Established by the European Commission
ERC AdG EUSTRONG
Bundesministerium für Bildung und Forschung

Structure of nuclei and dense matter in neutron stars

doi:10.1038/nature11188

The limits of the nuclear landscape

Jochen Erler[1,2], Noah Birge[1], Markus Kortelainen[1,2,3], Witold Nazarewicz[1,2,4], Erik Olsen[1,2], Alexander M. Perhac[1] & Mario Stoitsov[1,2]‡

~ 4000 ± 500 nuclei unknown, extreme neutron-rich

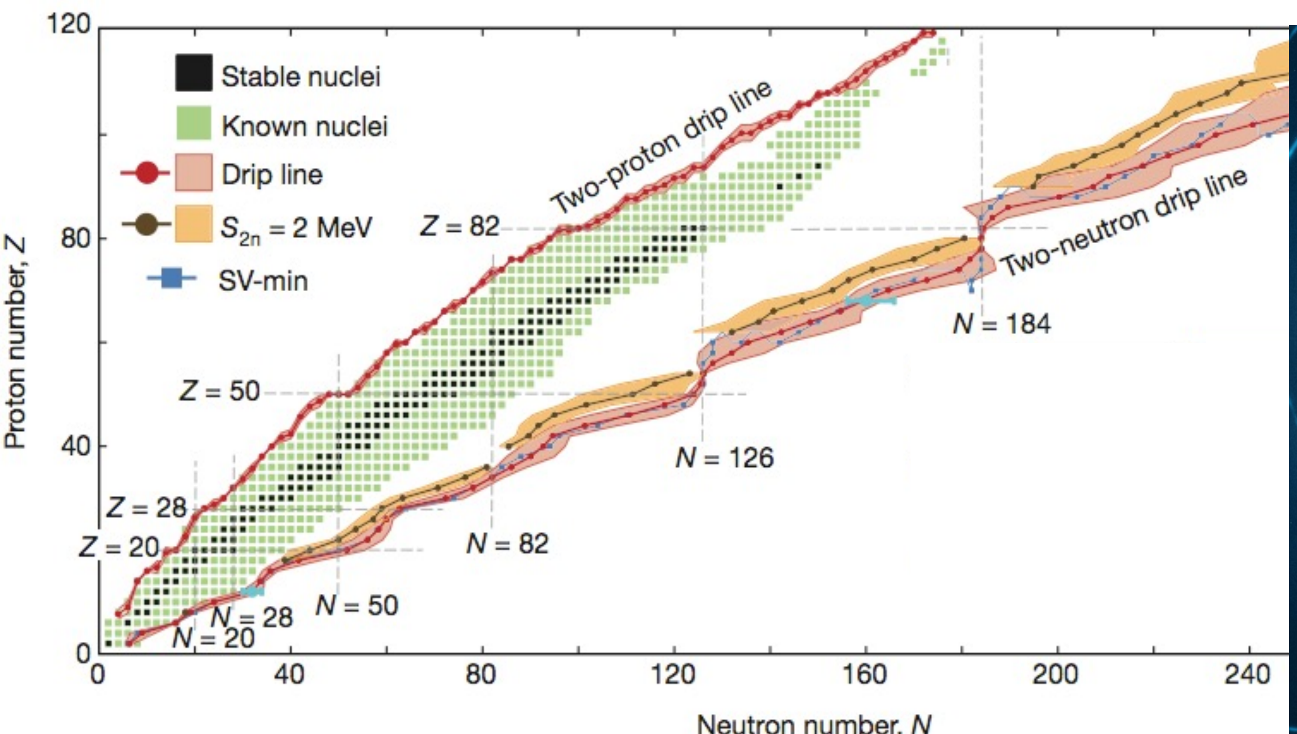

Extreme neutron-rich matter in neutron stars

Chiral effective field theory for nuclear forces

Systematic expansion (power counting) in low momenta $(Q/\Lambda_b)^n$

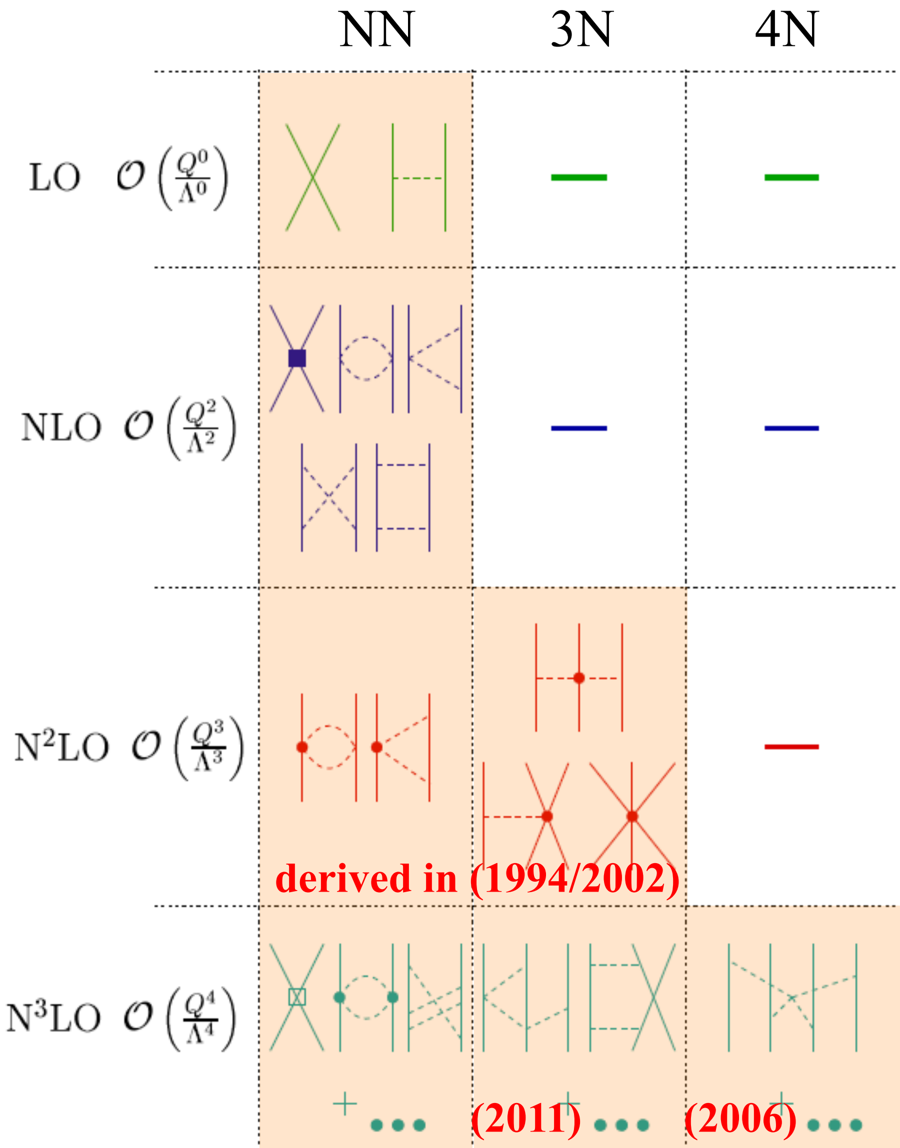

based on symmetries of strong interaction (QCD)

long-range interactions governed by pion exchanges

powerful approach for many-body interactions

all 3- and 4-neutron forces predicted to N^3LO

Tews, Krüger, Hebeler, AS, PRL (2013)

Weinberg (1990,91), van Kolck, Kaplan, Savage, Wise, Bernard, Epelbaum, Kaiser, Meißner,…

Great progress in ab initio calculations of nuclei

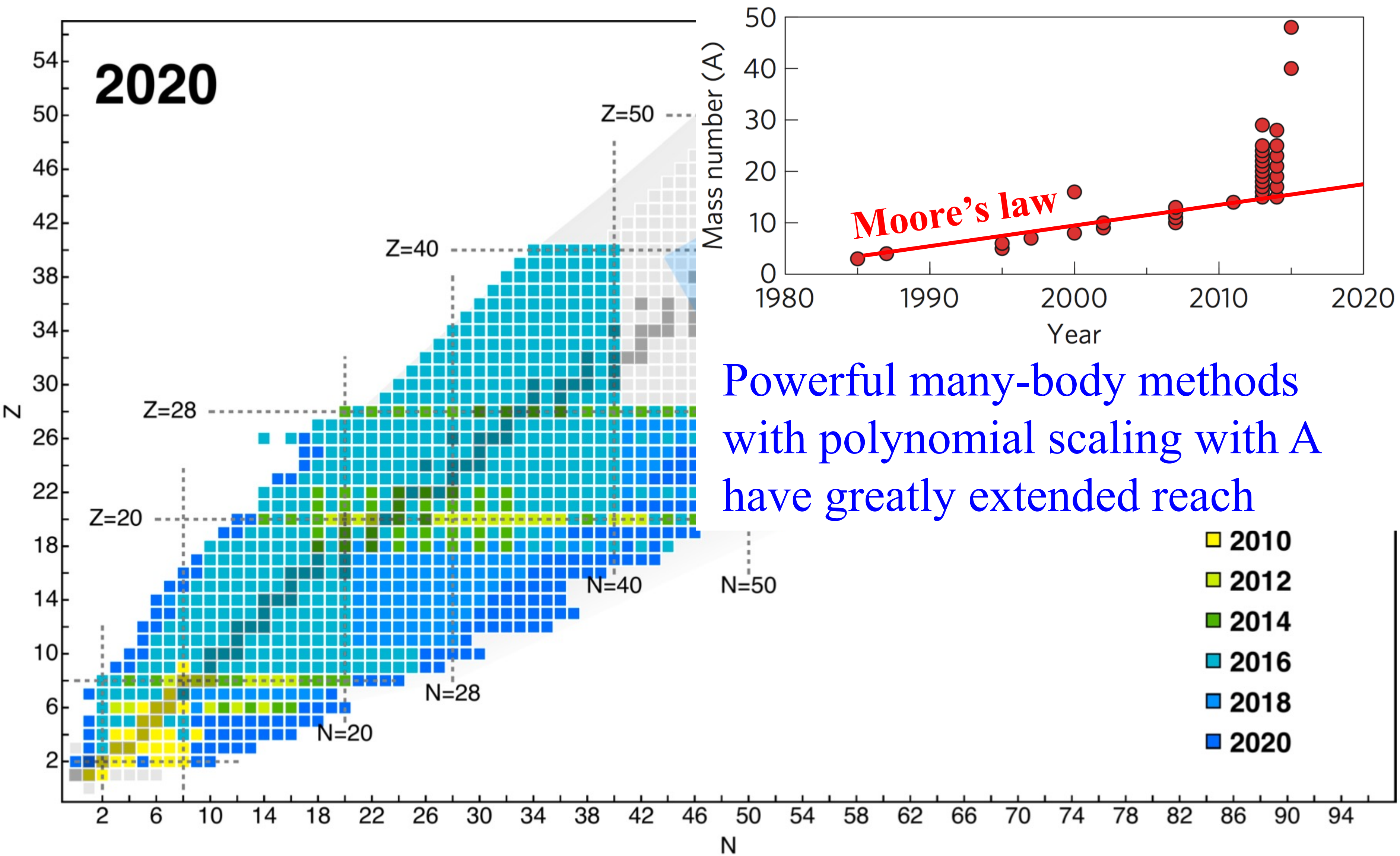

Powerful many-body methods with polynomial scaling with A have greatly extended reach

figures from Hagen et al., Nature Phys. (2016), Hergert (2020)

Great progress in ab initio calculations of nuclei

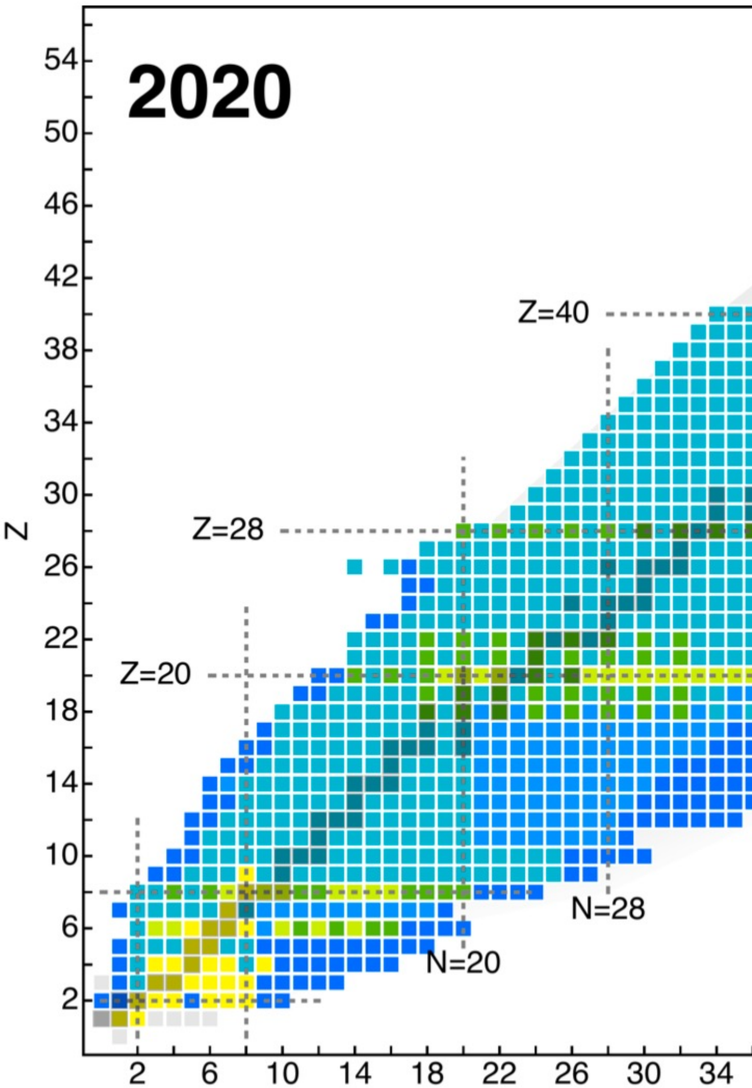

Chiral EFT interactions enable controlled solution of many-body Schrödinger eqn.

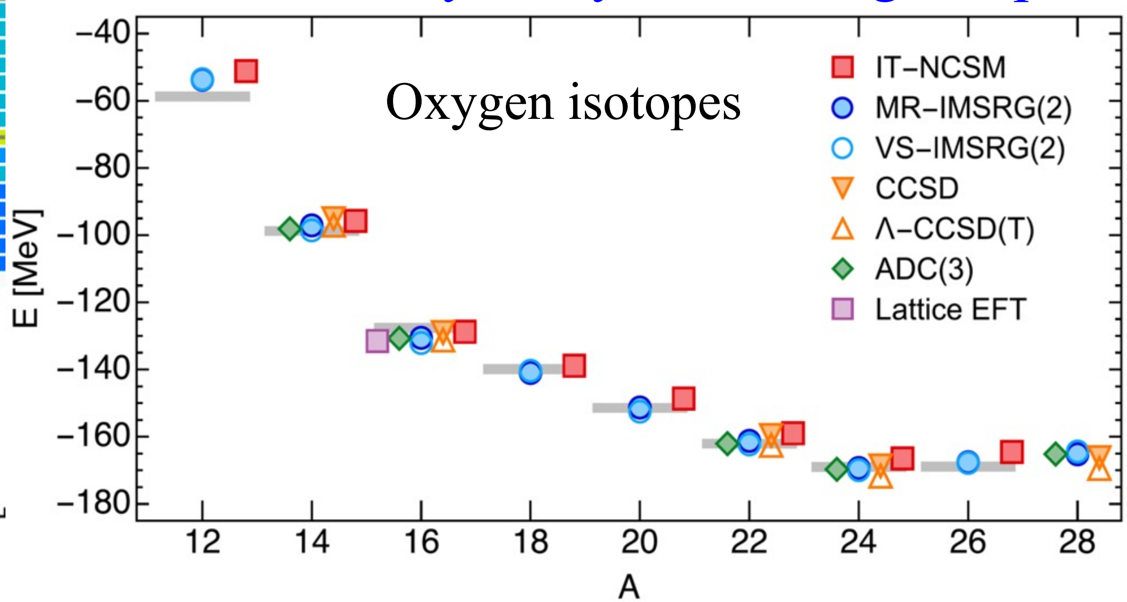

figures from Hagen et al., Nature Phys. (2016), Hergert (2020)

In-medium similarity renormalization group (IMSRG)

Tsukiyama, Bogner, AS, PRL (2011), Hergert et al., Phys. Rep. (2016)

continuous transformation to block-diagonal form (→ decoupling)

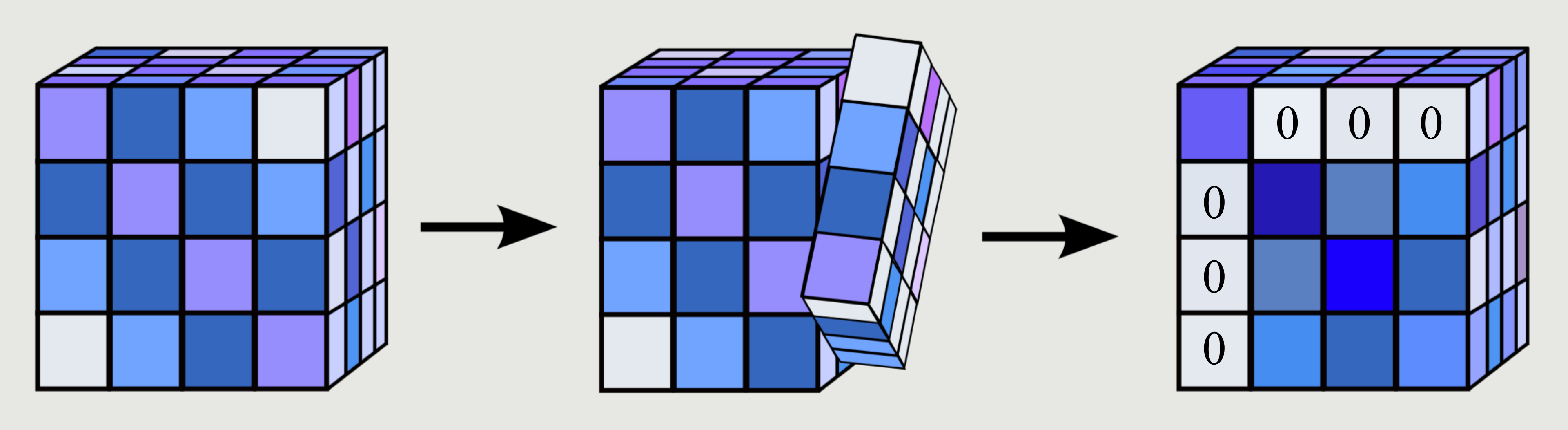

In-medium similarity renormalization group (IMSRG)

Tsukiyama, Bogner, AS, PRL (2011), Hergert et al., Phys. Rep. (2016)

RG flow equations to decouple higher-lying particle-hole states

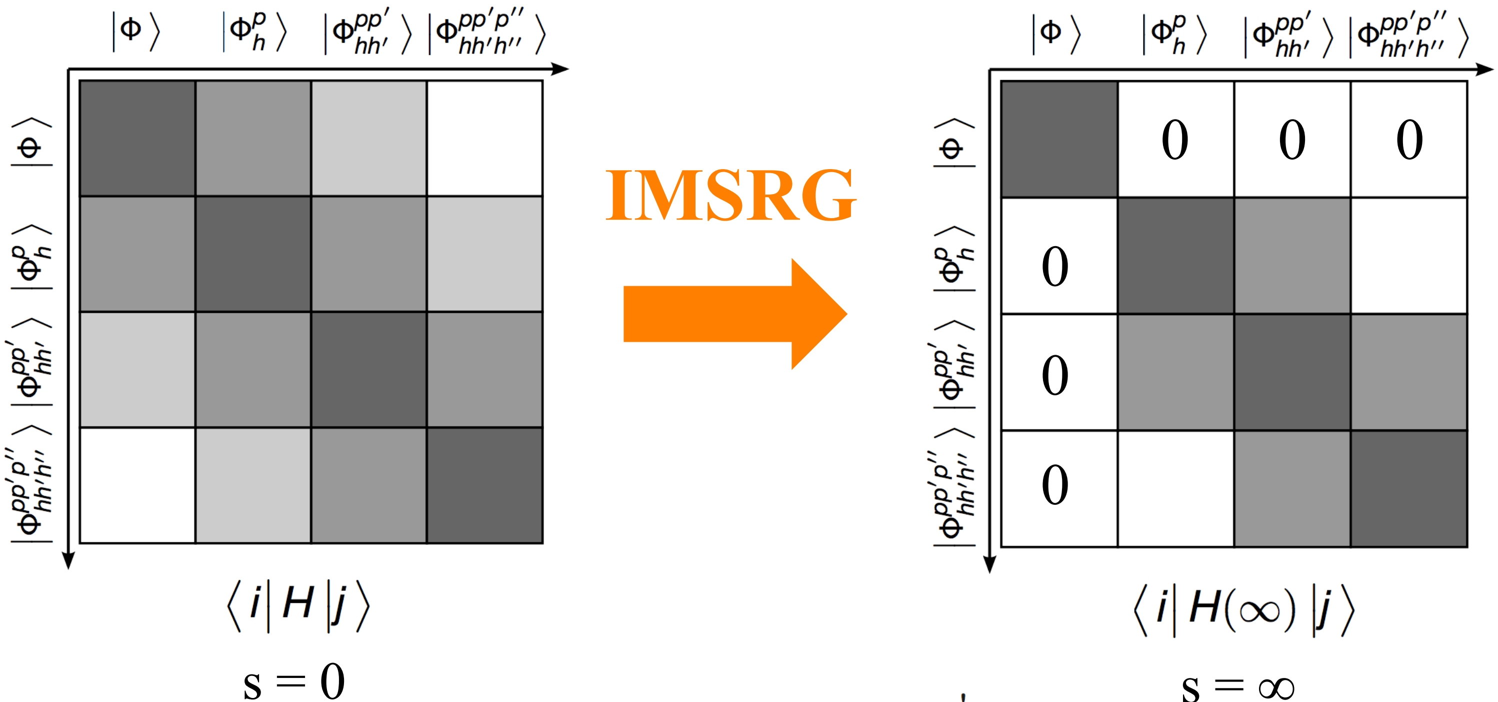

$$H(s) = U(s)H(0)U^{\dagger}(s)$$

In-medium similarity renormalization group (IMSRG)

Tsukiyama, Bogner, AS, PRL (2011), Hergert et al., Phys. Rep. (2016)

RG flow equations to decouple higher-lying particle-hole states

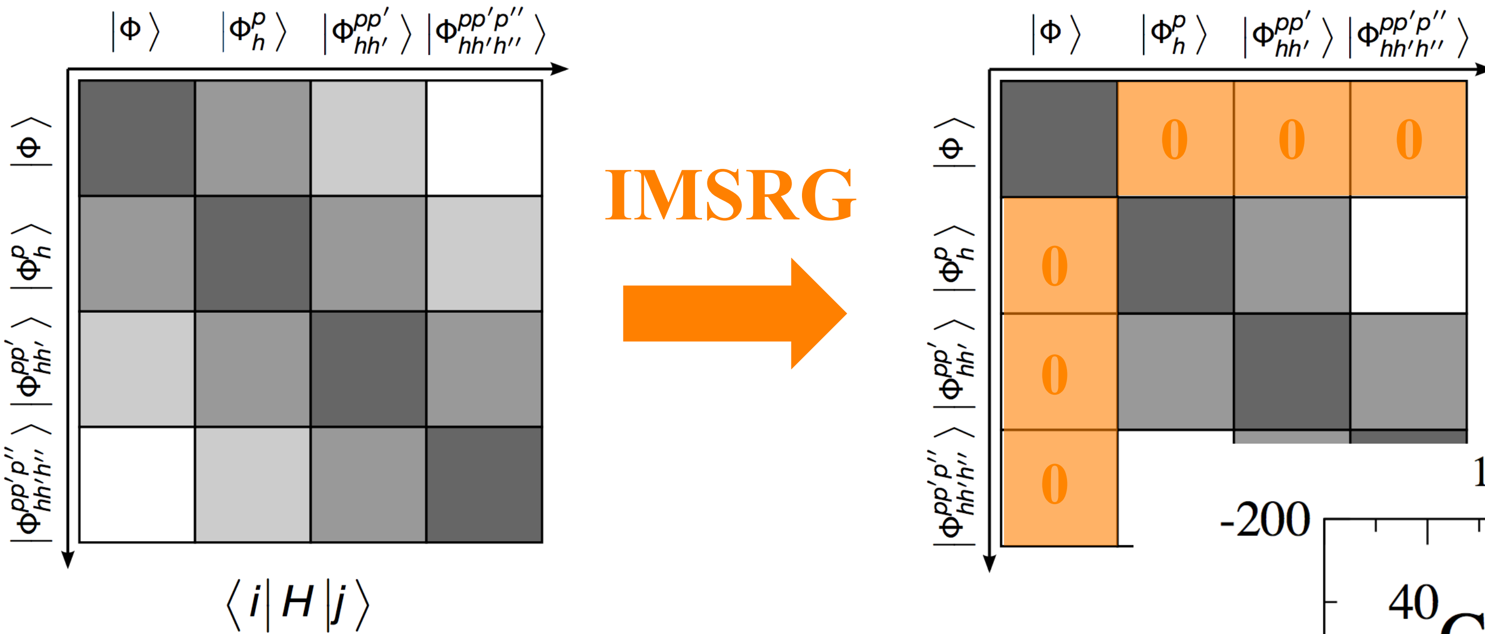

s = 0

$$H(s) = U(s)H(0)U^\dagger(s)$$

$$\frac{d}{ds}H(s) = [\eta(s), H(s)]$$

with generator $\eta = [H^d(s), H^{od}(s)]$

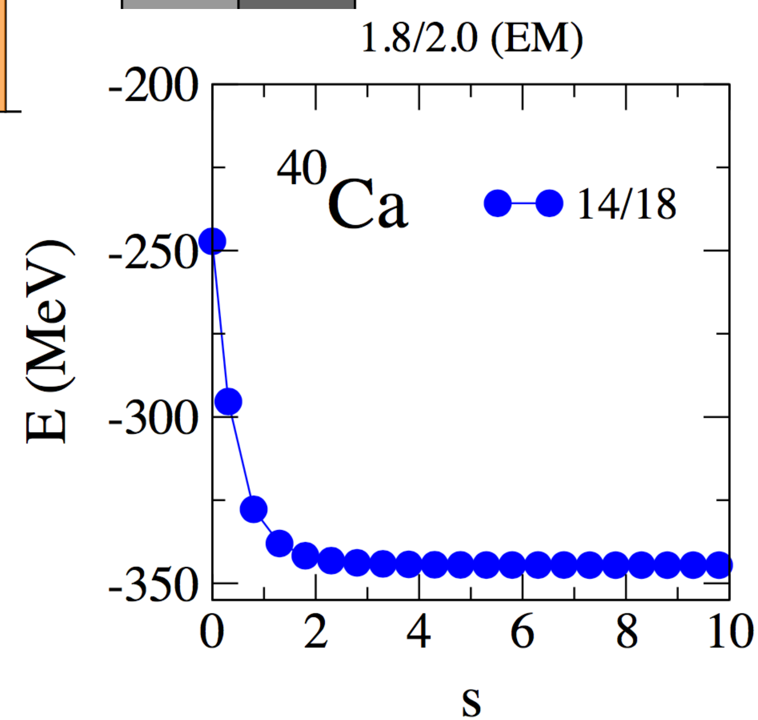

Nuclear landscape based on a chiral NN+3N interaction

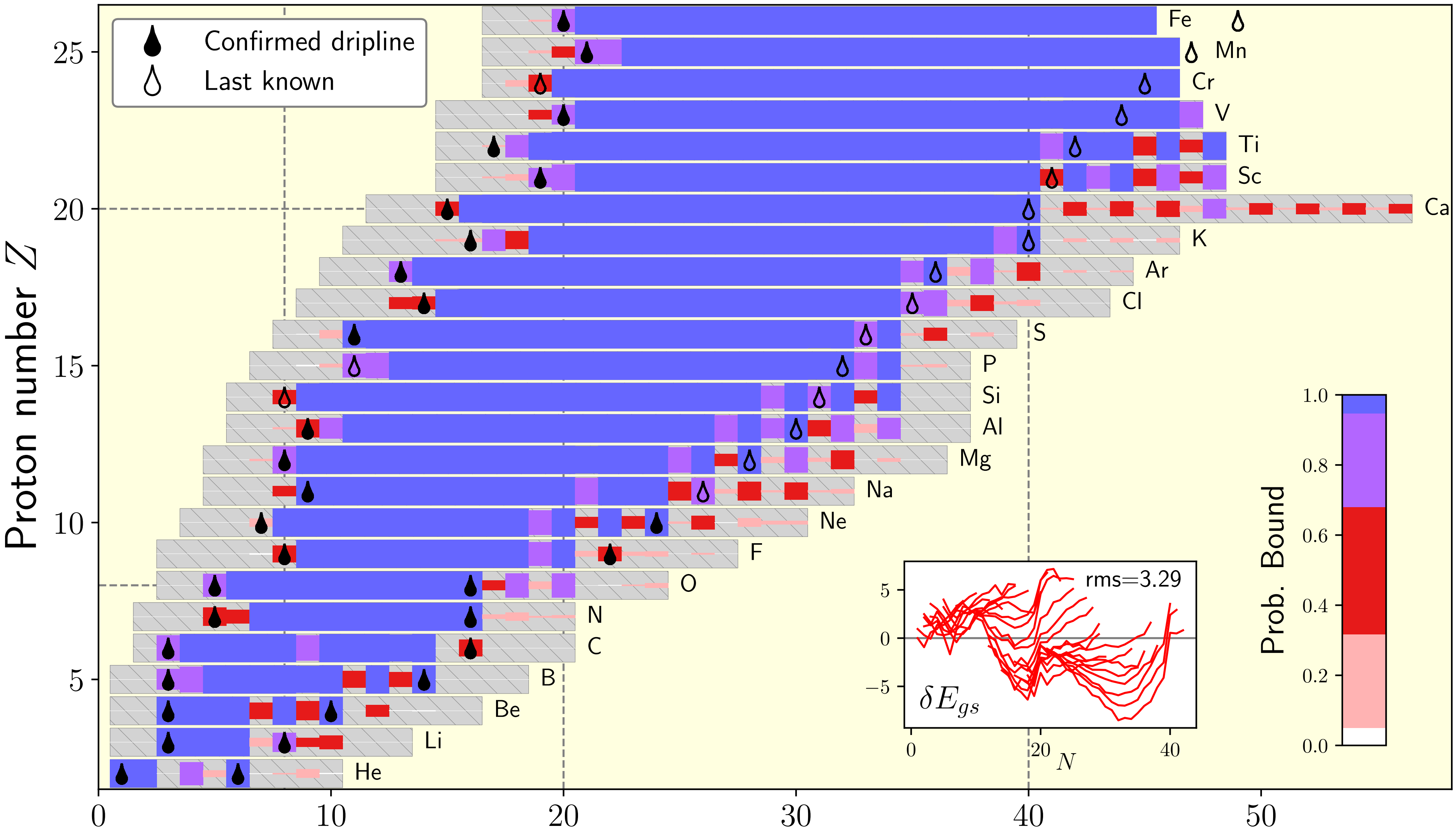

Stroberg, Holt, AS, Simonis, PRL (2021)

ab initio is advancing to global theories, limitations due to input NN+3N

Nuclear landscape based on a chiral NN+3N interaction

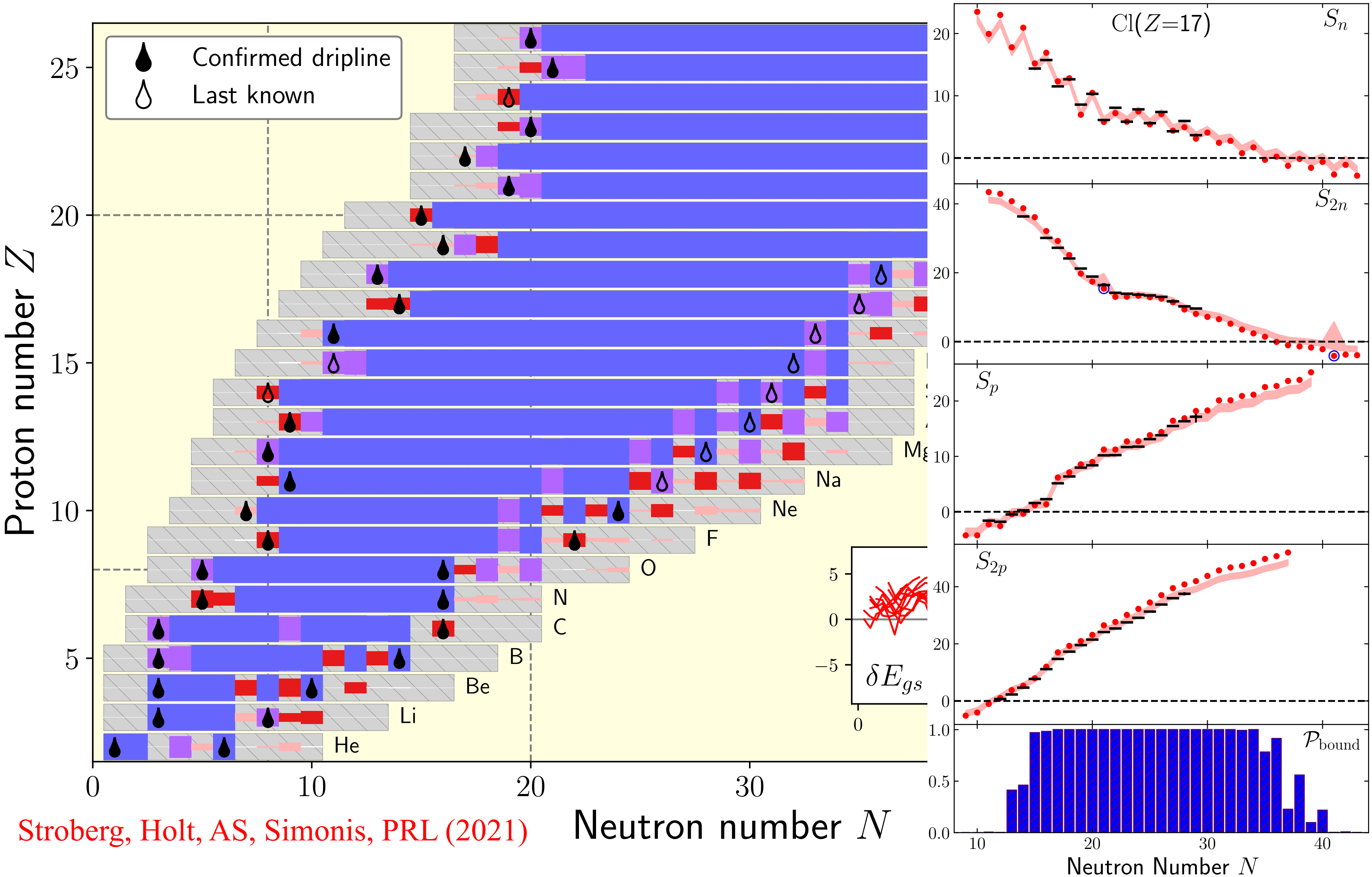

Stroberg, Holt, AS, Simonis, PRL (2021)

ab initio is advancing to global theories, limitations due to input NN+3N

Highlights from ISOLDE/CERN and RIBF/RIKEN

very active experiment-theory collaborations

pioneering $^{51\text{-}57}$Ca masses

Wienholtz et al., Nature (2013)
Michimasa et al., PRL (2019)

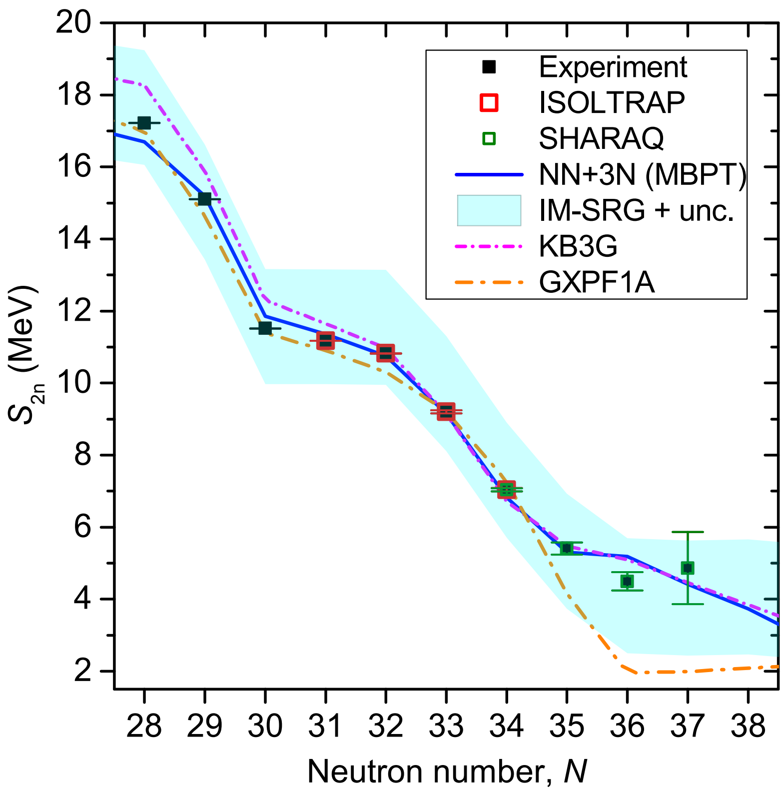

importance of 3N interactions for neutron-rich shell structure

discovery of doubly magic ^{78}Ni

Taniuchi et al., Nature (2019)

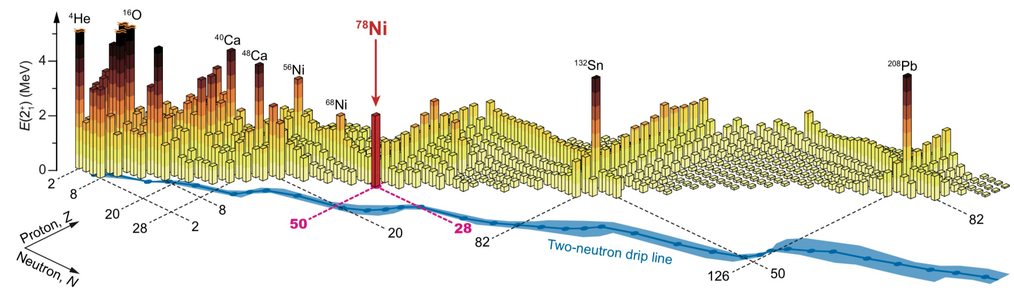

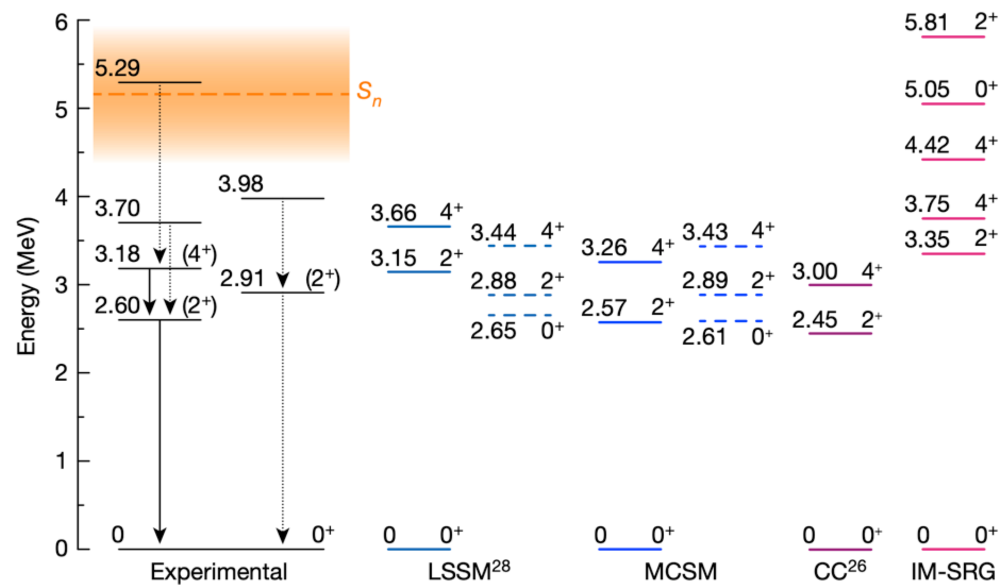

First ab initio calculations of ^{208}Pb

Hu, Jiang, Miyagi, Sun et al., Nature Phys. (2022)

enabled by 3N advances

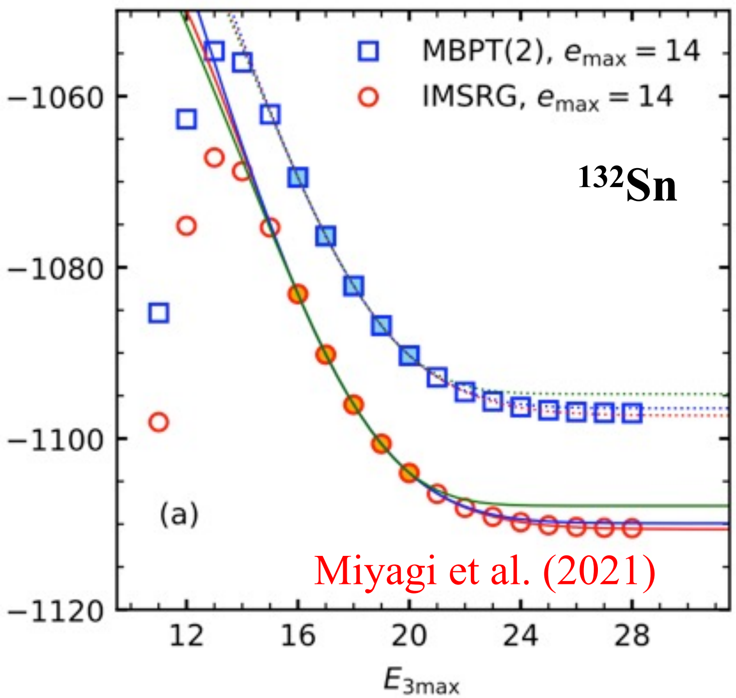

statistical methods via history matching
to explore uncertainties in NN+3N

predicted **neutron skin of ^{208}Pb**
agrees with most experiments

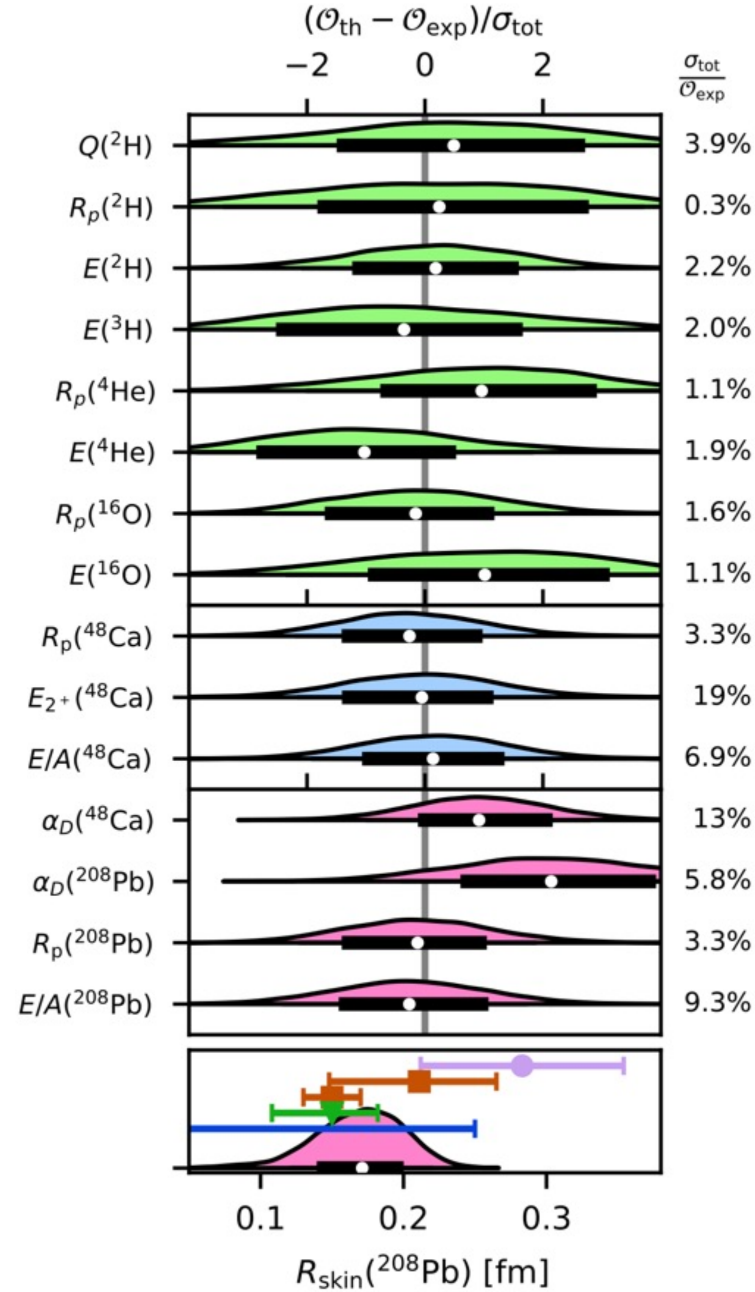

Extreme matter in neutron stars

governed by the same strong interactions:
chiral EFT sets pressure of first few km to inside

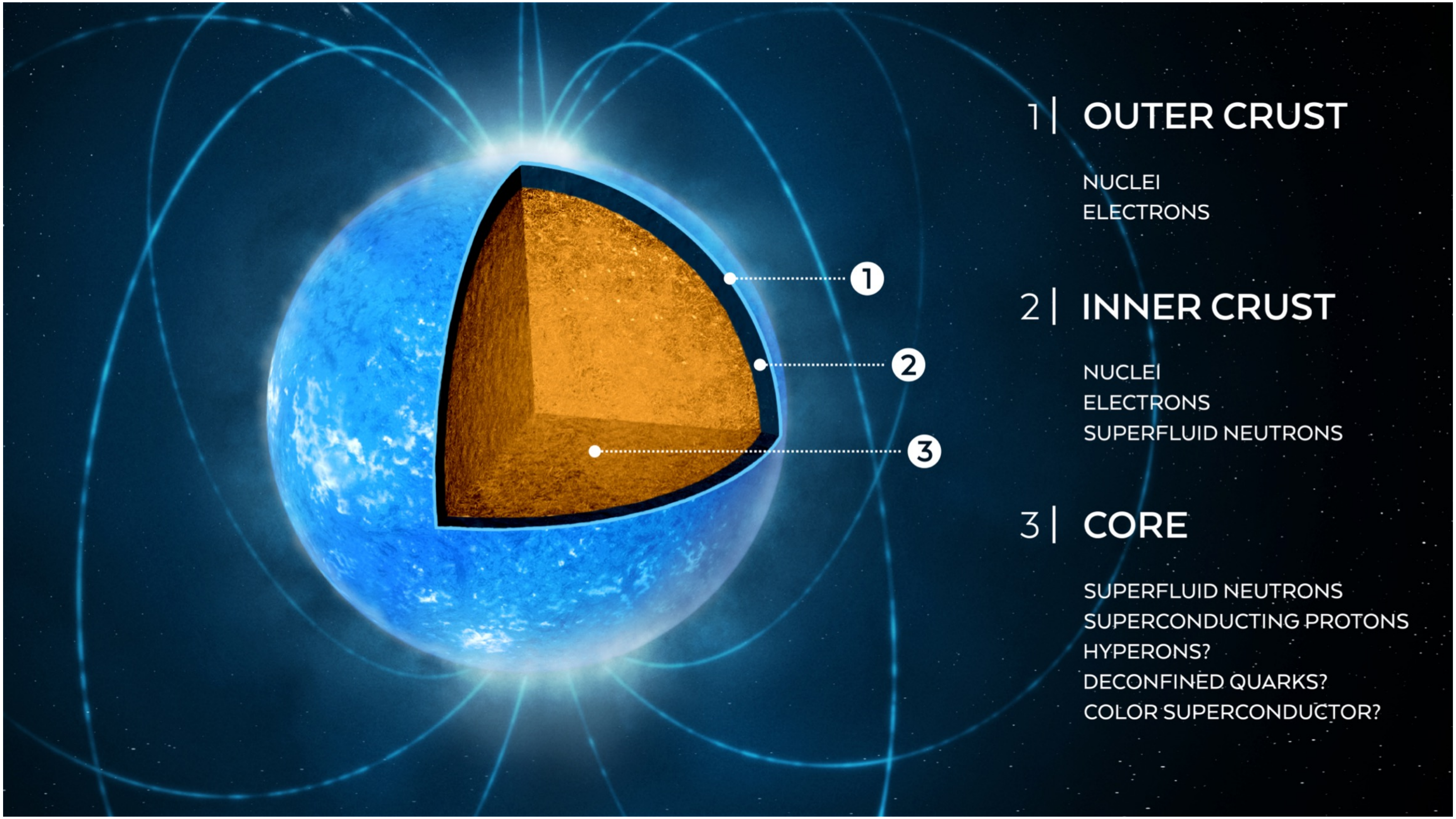

Watts et al., RMP (2016)

Chiral EFT calculations of dense matter

good agreement up to saturation density for neutron matter including NN, 3N, 4N interactions up to N^3LO

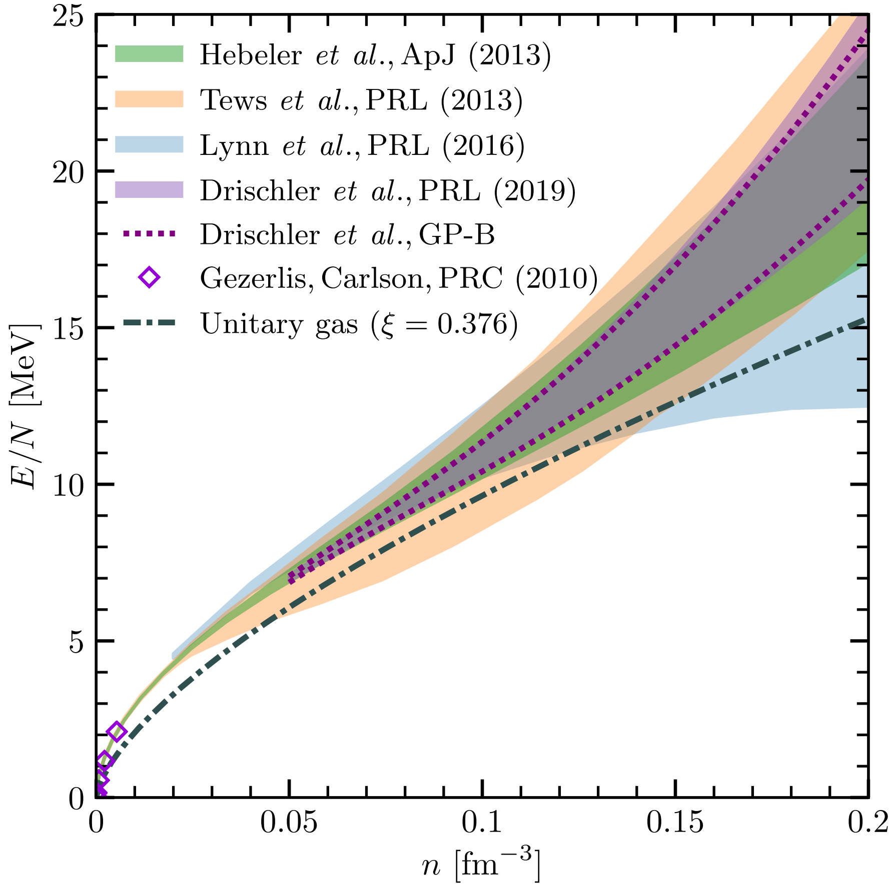

from Huth, Wellenhofer, AS, PRC (2021)

slope determines pressure of neutron matter

EOS for arbitrary proton fraction and finite temperature using Gaussian Process emulator

Keller, Hebeler, AS, PRL (2023)

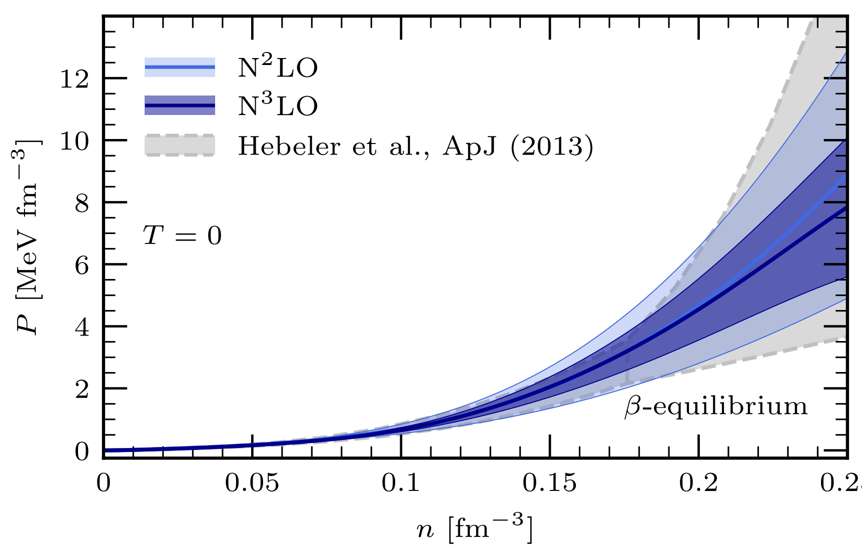

Neutron star masses

from Jim Lattimer

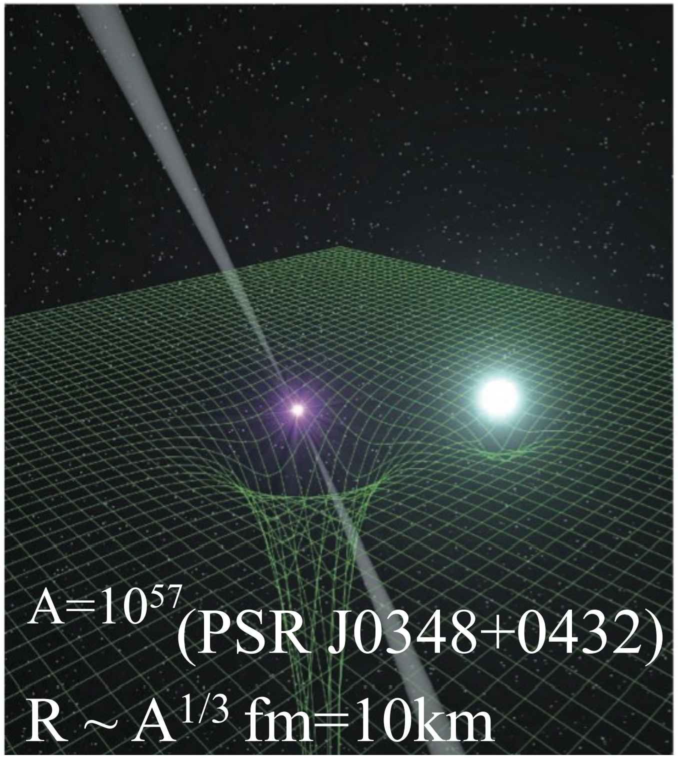

three 2 M_{sun} neutron stars obs.

J1614: Demorest et al., Nature (2010),

J0348: Antoniadis et al., Science (2013),

J0740: 2.08±0.07 M_{sun} Fonseca et al., (2021)

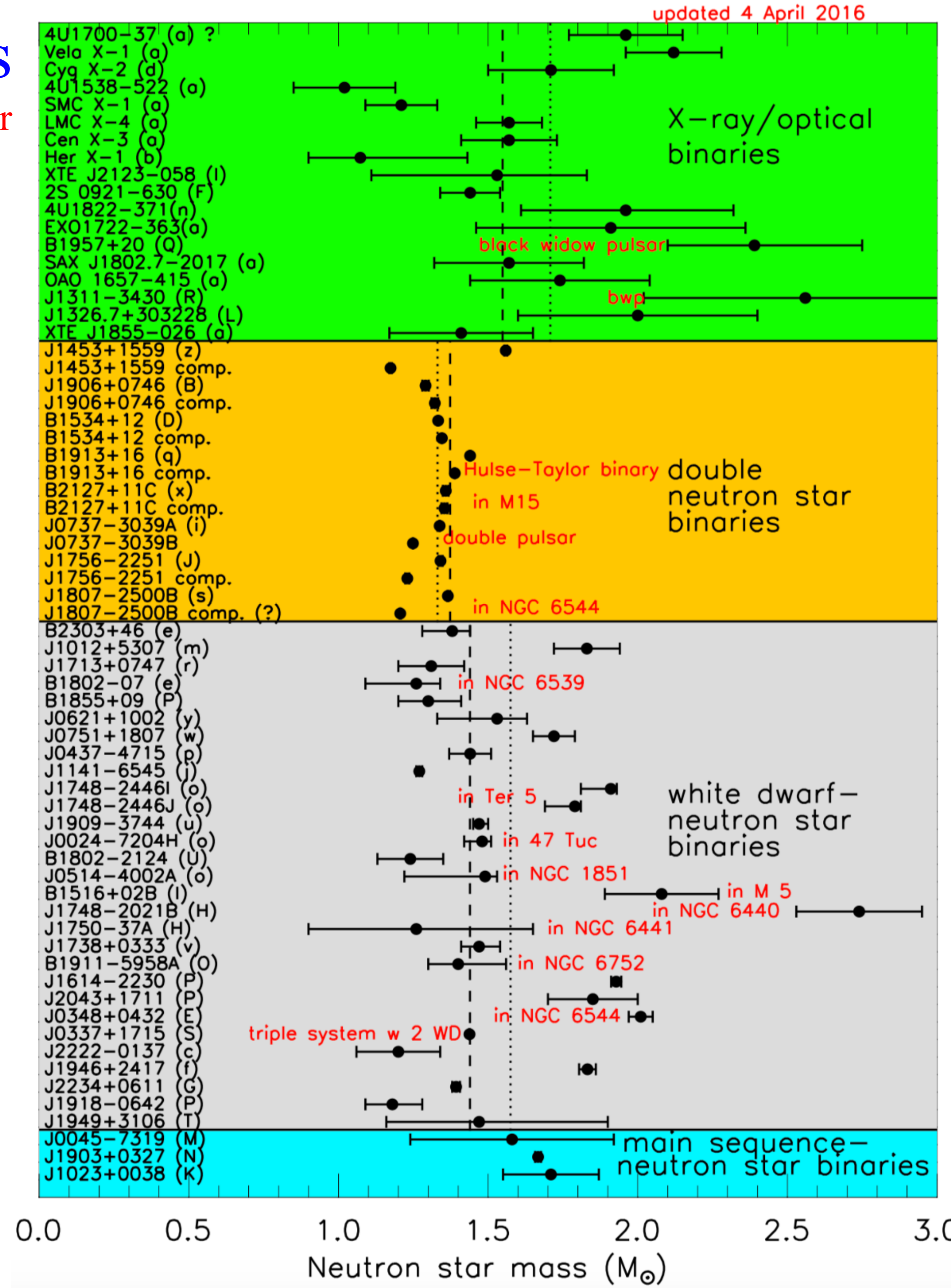

Neutron star radius

chiral EFT + general EOS extrapolation based on causality + 2 M_{sun} stars

predicted neutron star radii: 9.7 - 13.9 km for M=1.4 M_{sun}

Hebeler, Lattimer, Pethick, AS, PRL (2010), ApJ (2013)

consistent with LIGO/Virgo

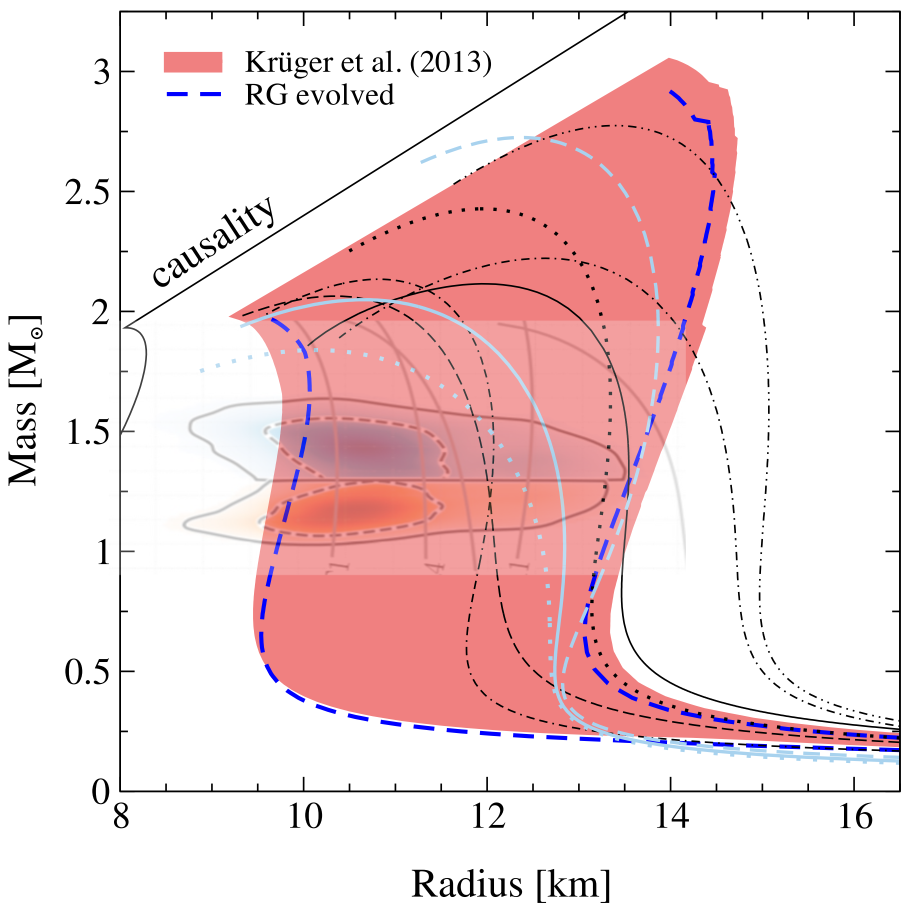

GW170817: Measurements of neutron star radii and equation of state

The LIGO Scientific Collaboration and The Virgo Collaboration

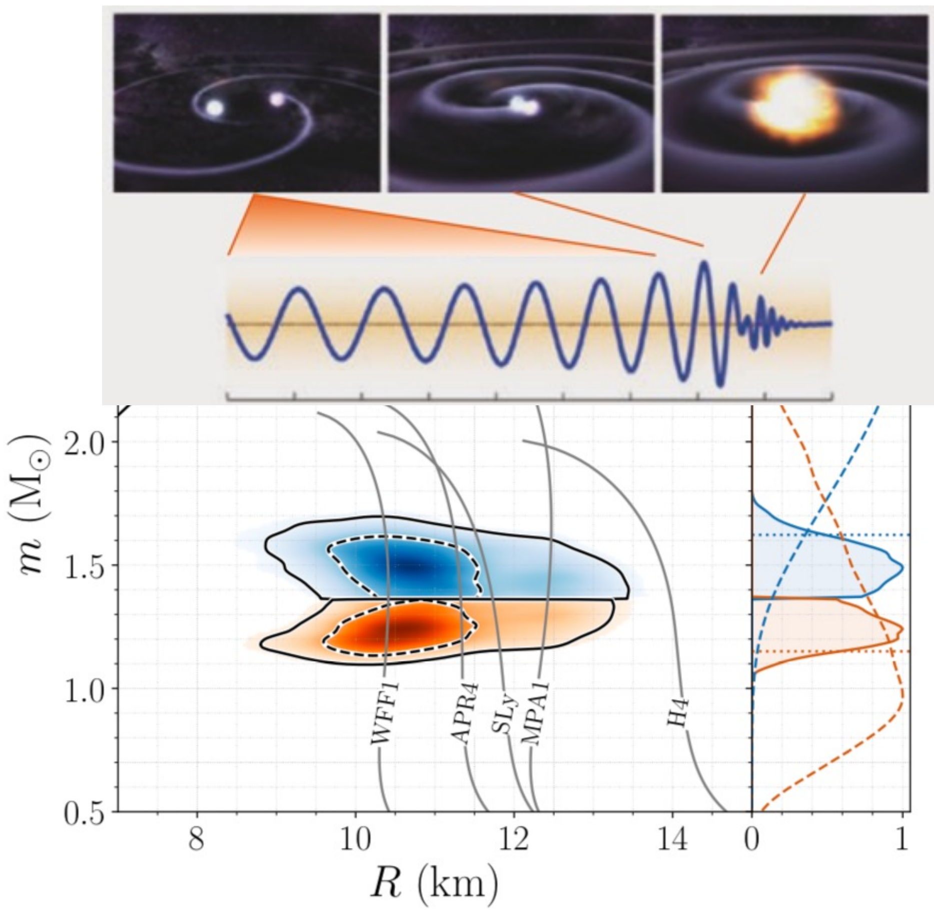

NICER results

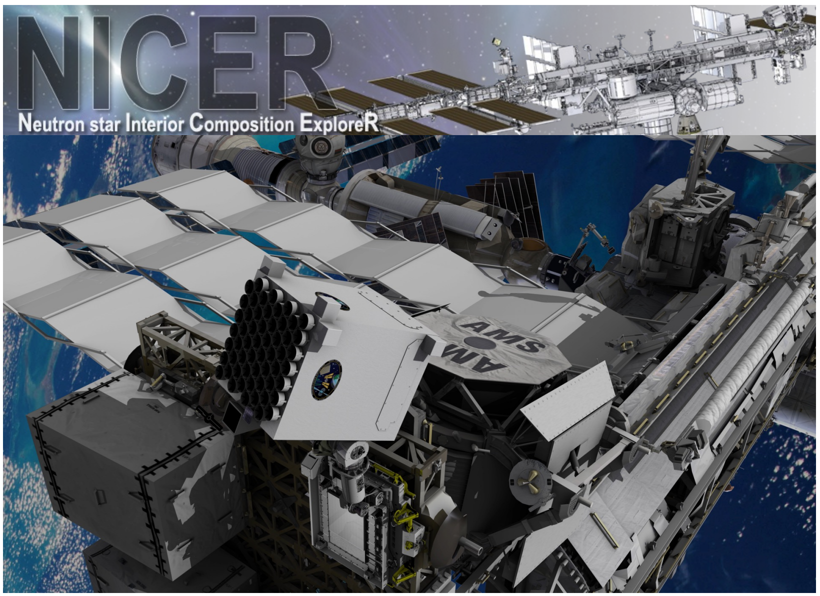

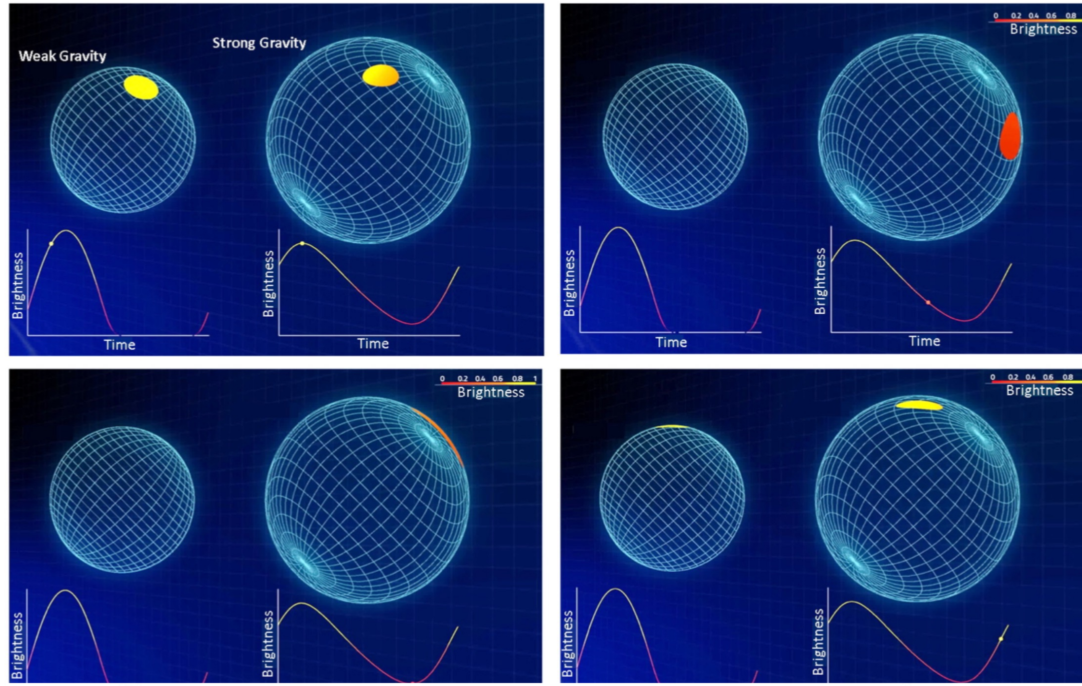

Neutron star radius from pulse profile modeling

J0030 and J0740
here: Amsterdam analysis
Riley et al., ApJL (2019), (2021)

similar results from Illinois-Maryland analysis
Miller et al., ApJL (2019), (2021)

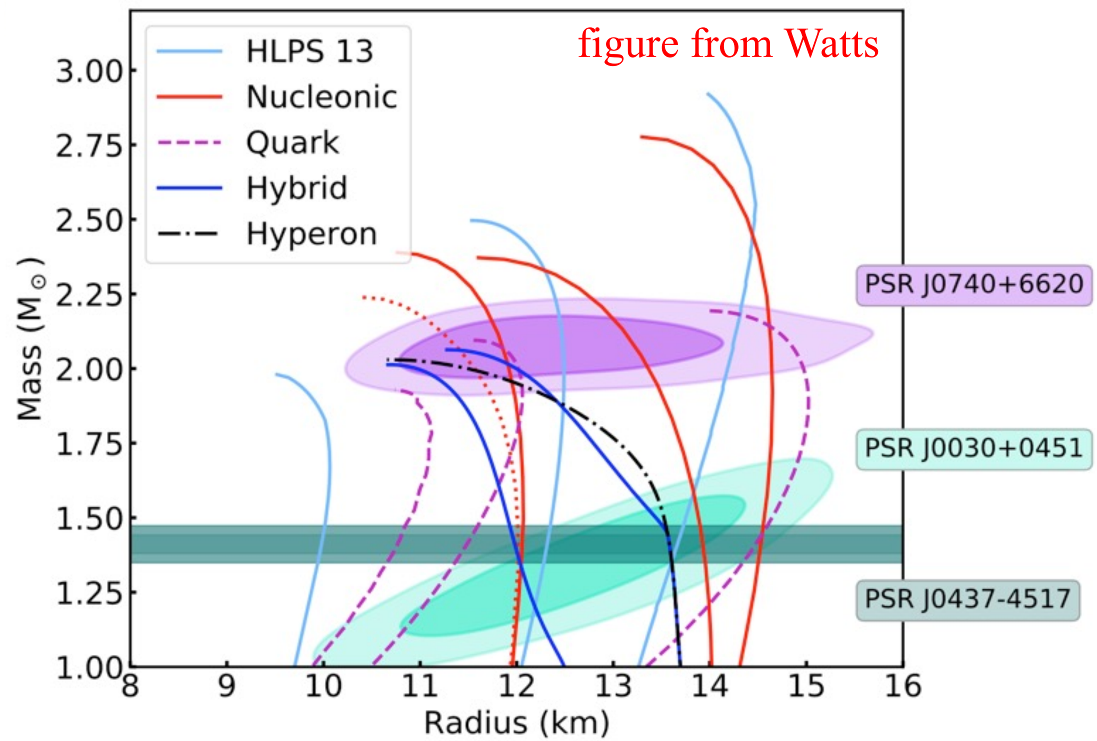

Combined LIGO/Virgo and NICER constraints

Raaijmakers et al., ApJL (2020), (2021)

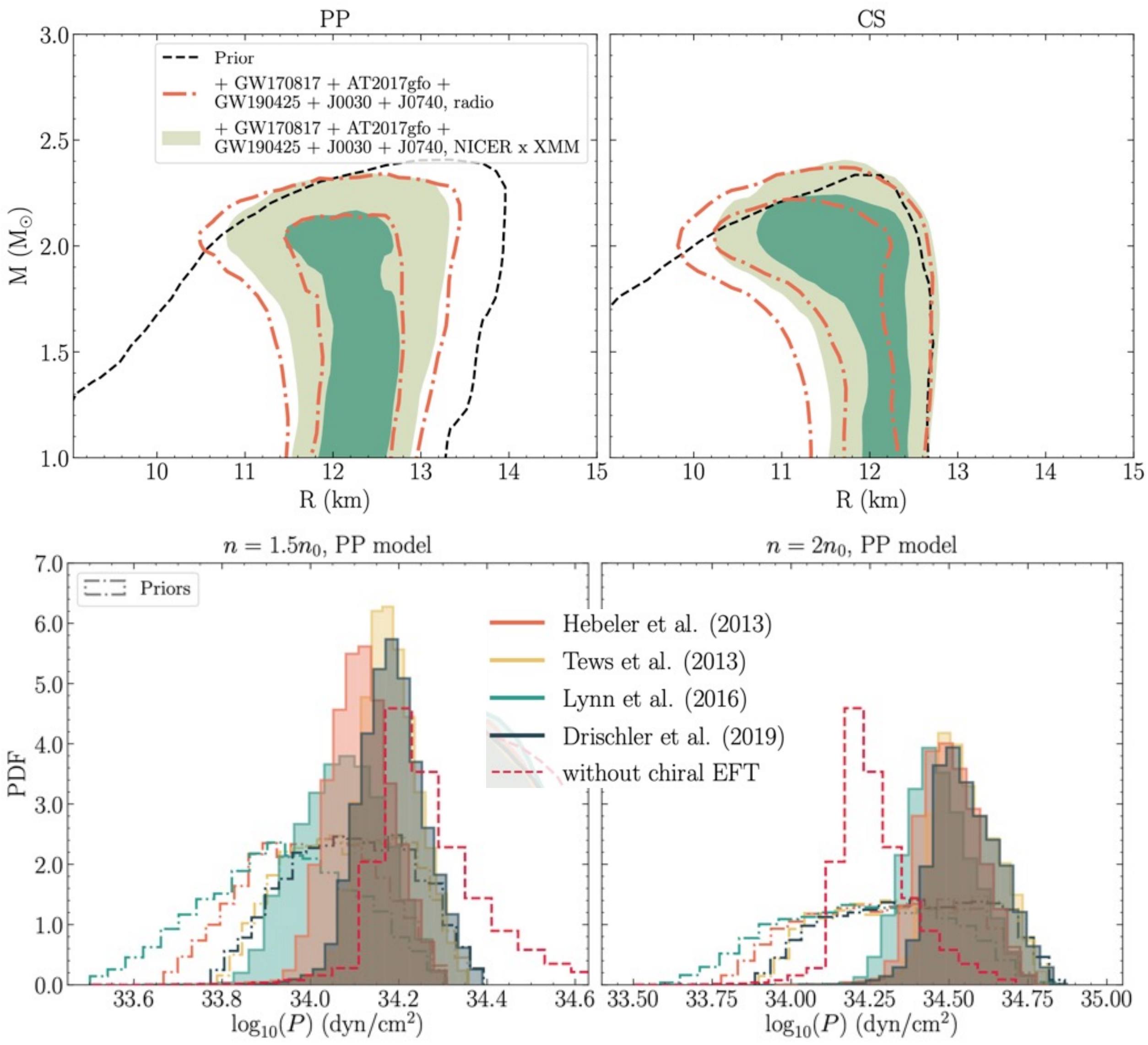

neutron star radius ~12 km

pressure posteriors at 1.5 and 2 n_0 → astro prefers higher pressures

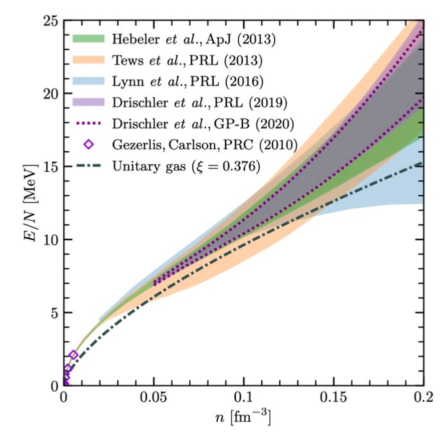

Constraints from heavy-ion collisions Huth, Pang et al., Nature (2022)

inclusion of HIC constraints prefers higher pressures, similar to NICER, overall remarkable consistency with chiral EFT and astro constraints

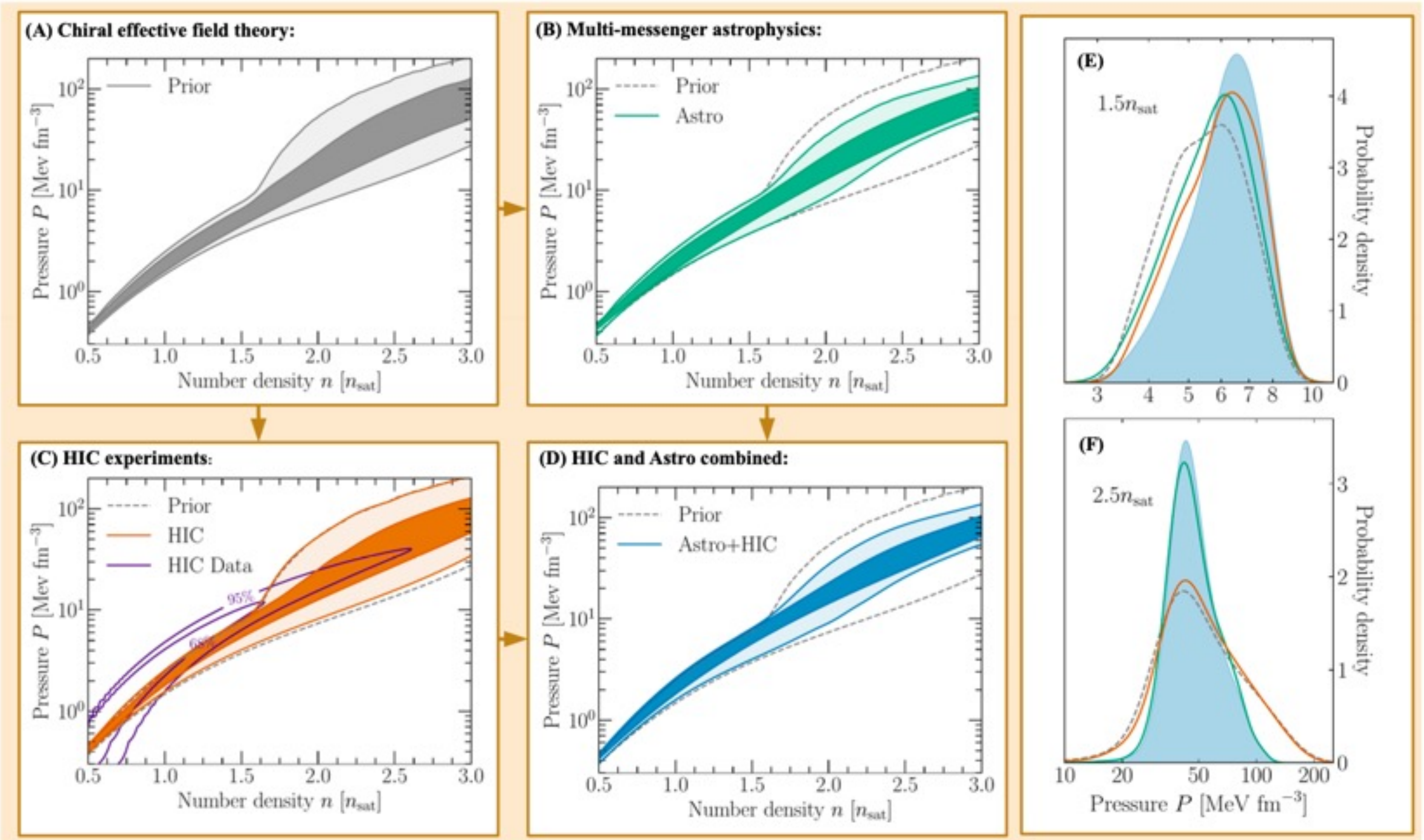

EOS for arbitrary proton fraction and temperature

Keller, Hebeler, AS, PRL (2023)

based on chiral EFT NN+3N interactions to N^{3}LO

order-by-order EFT uncertainties $\Delta X^{(j)} = Q \cdot \max\left(|X^{(j)} - X^{(j-1)}|, \Delta X^{(j-1)}\right)$

(small) many-body uncertainties at MBPT(3)

excellent reproduction of free energy data by Gaussian process

agrees with model-indep. virial EOS Horowitz, AS, NPA (2006) at low densities

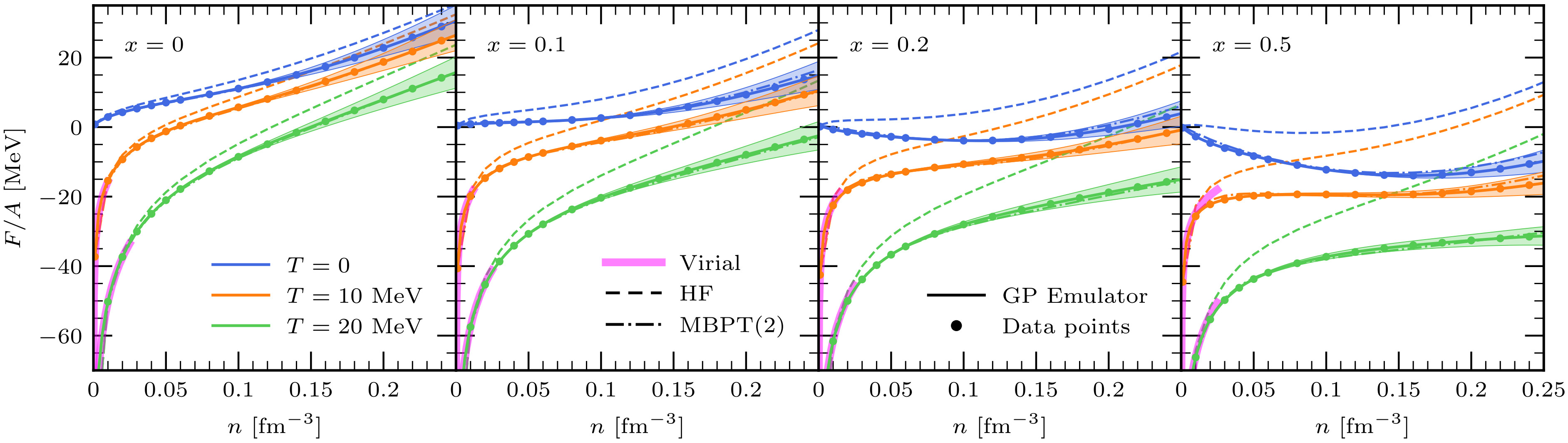

EOS for arbitrary proton fraction and temperature

Keller, Hebeler, AS, PRL (2023)

GP emulator to calculate pressure (thermodyn. consistent derivatives)

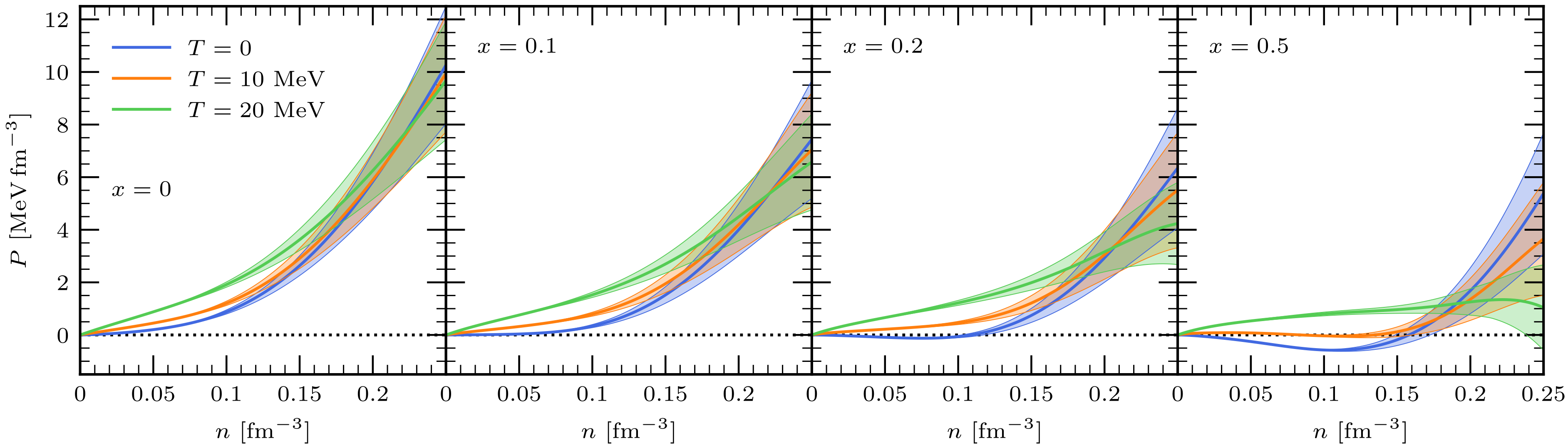

pressure isothermals cross at higher densities → negative thermal expansion

thermal part of pressure decreases with increasing density, observed for different chiral orders, cutoffs and interactions

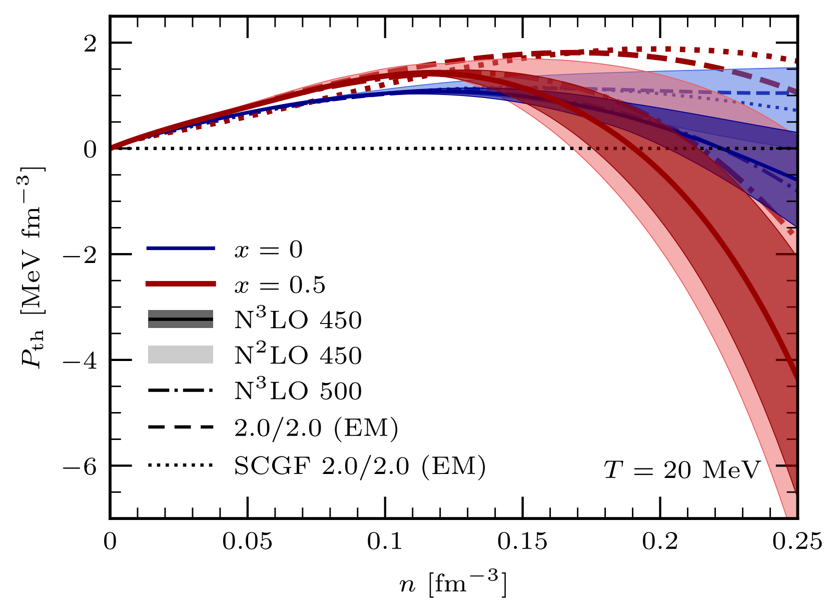

EOS for neutron star matter in beta equilibrium

Keller, Hebeler, AS, PRL (2023)

use GP emulator to access arbitrary proton fraction,
solve for beta equilibrium

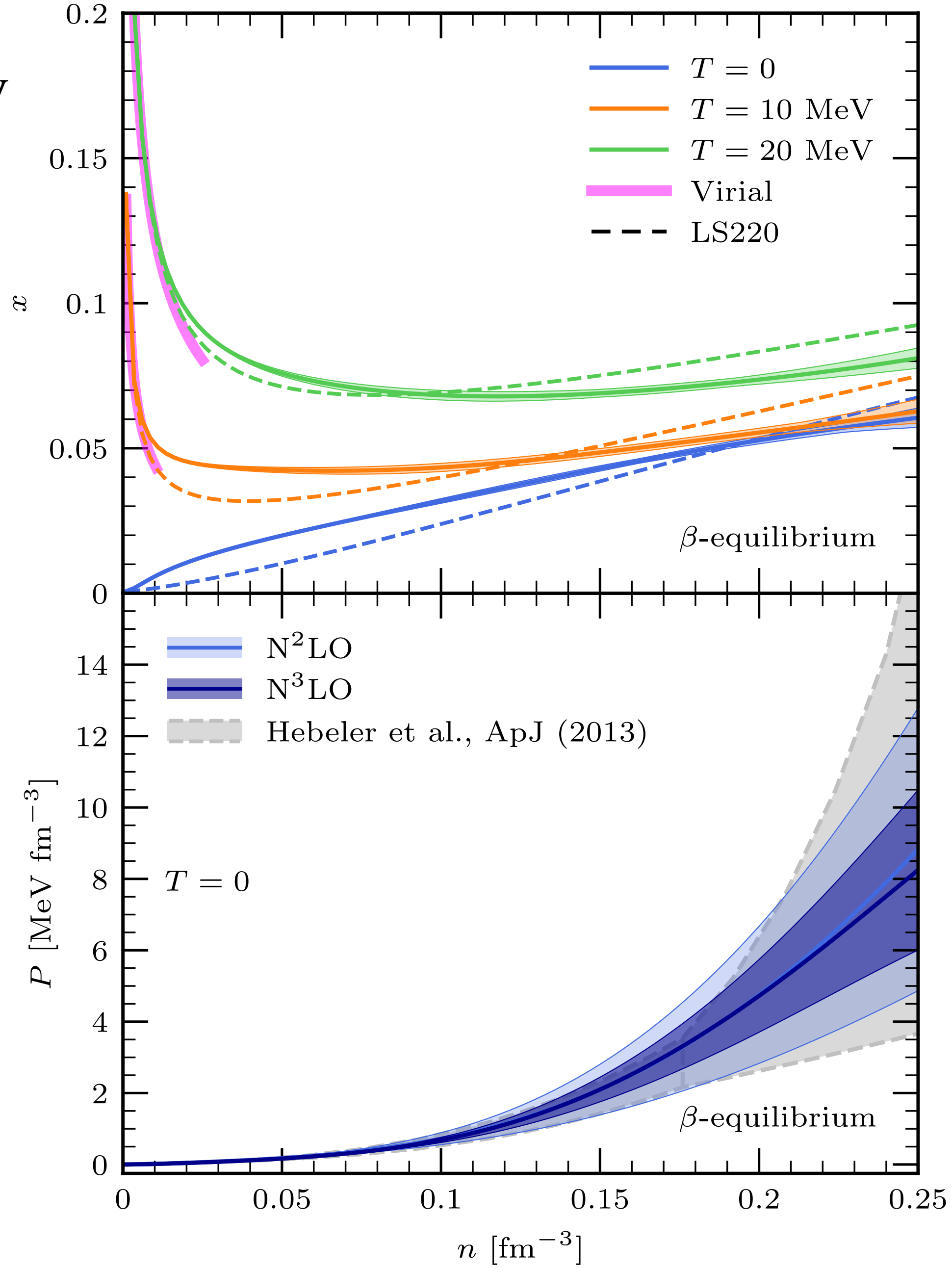

EOS of neutron star matter
at N^{2}LO and N^{3}LO,
no indication of EFT breakdown

N^{3}LO band prefers higher
pressures, improvement over
older calculations

Chiral EFT for coupling to electroweak interactions

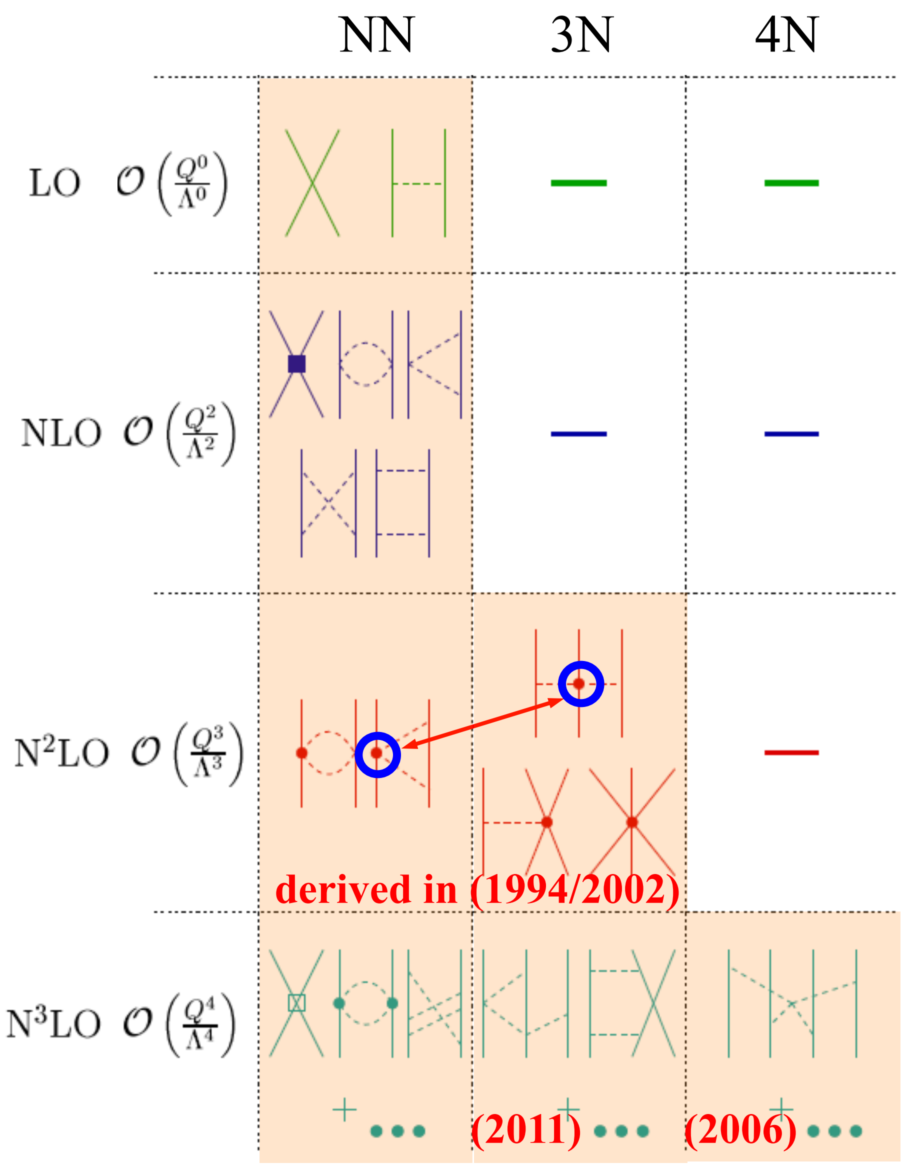

axial-vector currents (beta decays)

one-body currents at Q^0 and Q^2

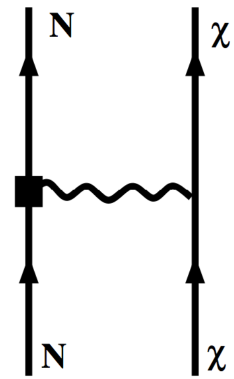

+ two-body currents at Q^3

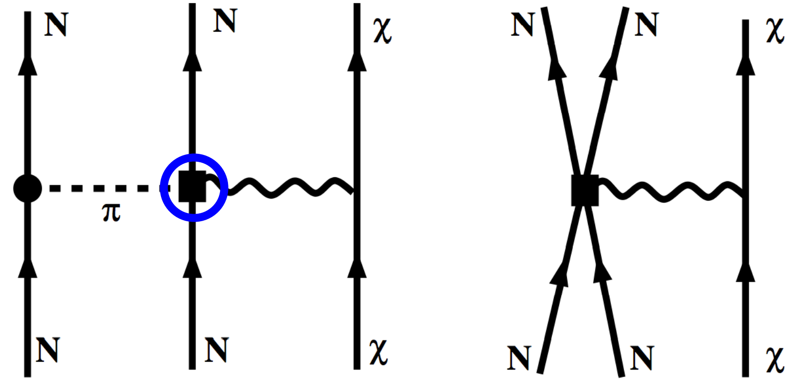

same couplings in forces and currents

Chiral EFT for coupling to electroweak interactions

consistent electroweak one- and two-body currents

magnetic properties of light nuclei

Pastore et al. (2012-)

B(M1) of ^{6}Li Gayer et al., PRL (2021)

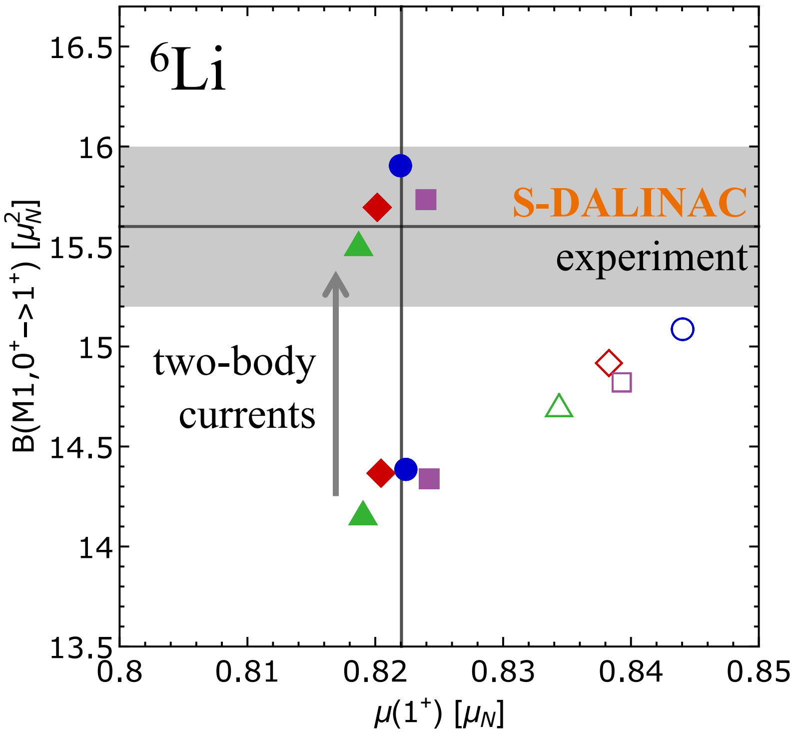

Gamow-Teller beta decay of ^{100}Sn

Gysbers et al., Nature Phys. (2019)

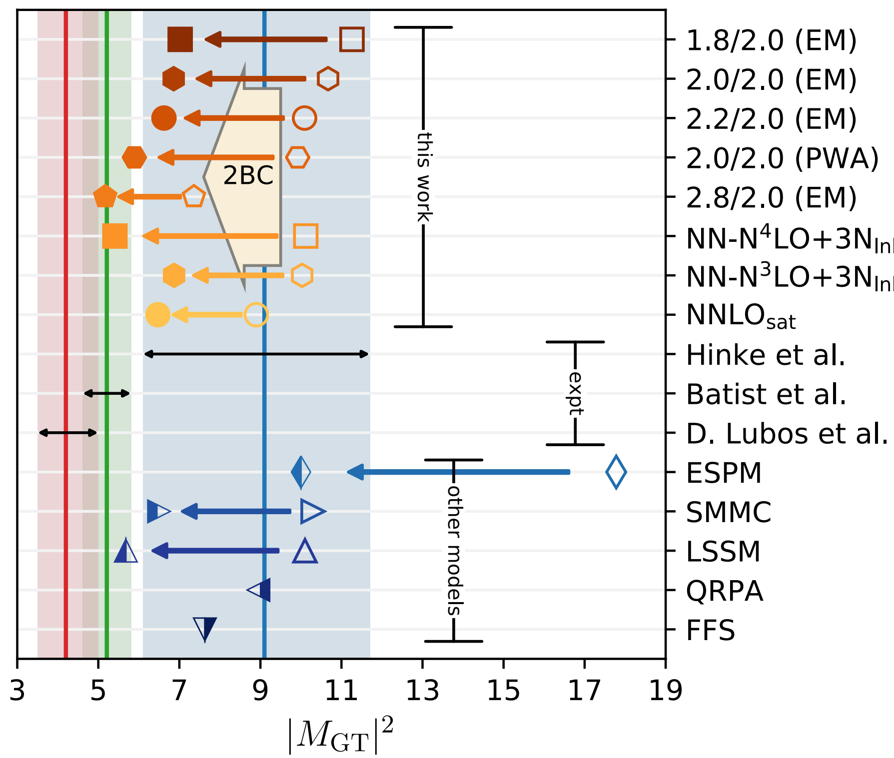

two-body currents (2BC) key for quenching puzzle of beta decays

Nuclear physics of DM direct detection and CEνNS

developed general framework for WIMPs coupling to nuclei
based on chiral EFT including two-body currents
Klos, Hoferichter et al., PRD (2013-2019)

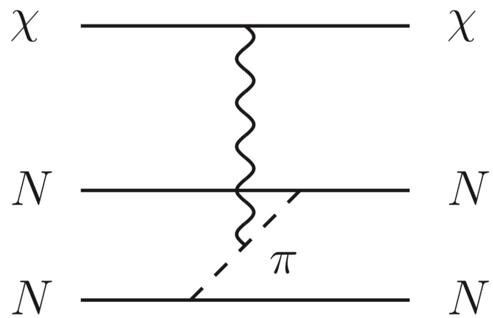

first limits for WIMP pion coupling
with XENON1T collaboration
Aprile et al., PRL (2019)
partially coherent between SI and SD

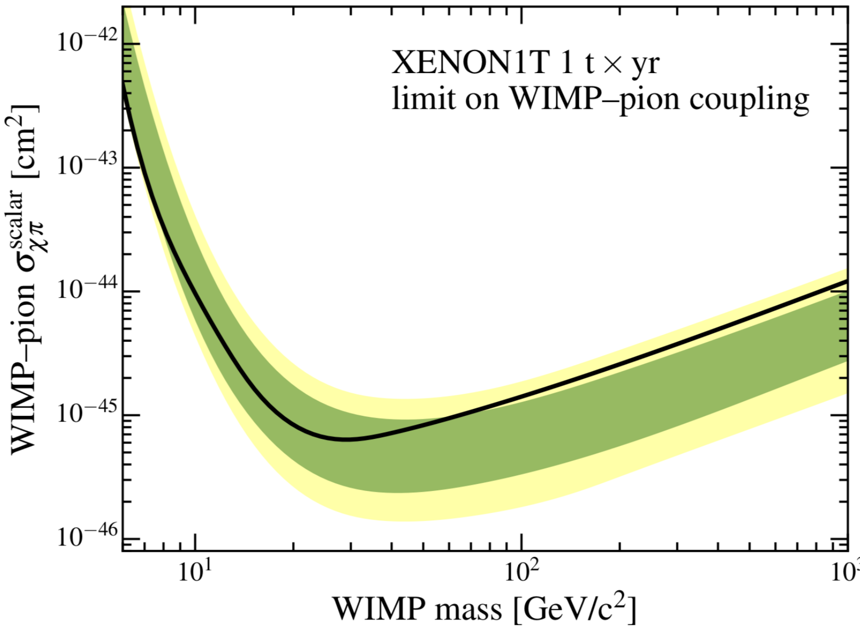

developed consistent chiral EFT responses for CEνNS
Hoferichter et al., PRD (2022)

Summary

Thanks to: **ab initio:** S. Bacca, S. Bogner, G. Hagen, K. Hebeler, M. Heinz, J.D. Holt, T. Miyagi, T. Papenbrock, J. Simonis, R. Stroberg, A. Tichai; **EOS:** T. Dietrich, C. Drischler, S. Greif, S. Huth, J. Lattimer, J. Keller, P. Pang, C. Pethick, G. Raaijmakers, I. Tews, A. Watts; **currents:** C. Brase, M. Hoferichter, J. Menéndez

Chiral EFT combined with powerful many-body methods enable great progress for ab initio calculations of nuclei and matter

Reliable EOS up to ~1.5 n_0 with controlled uncertainties to explore neutron stars + high-density information from astro

Response functions for DM/CEν-nucleus scattering based on chiral EFT currents, incorporate what we know about QCD

Symmetry energy vs. L parameter based on Lattimer, Lim, ApJ (2013)

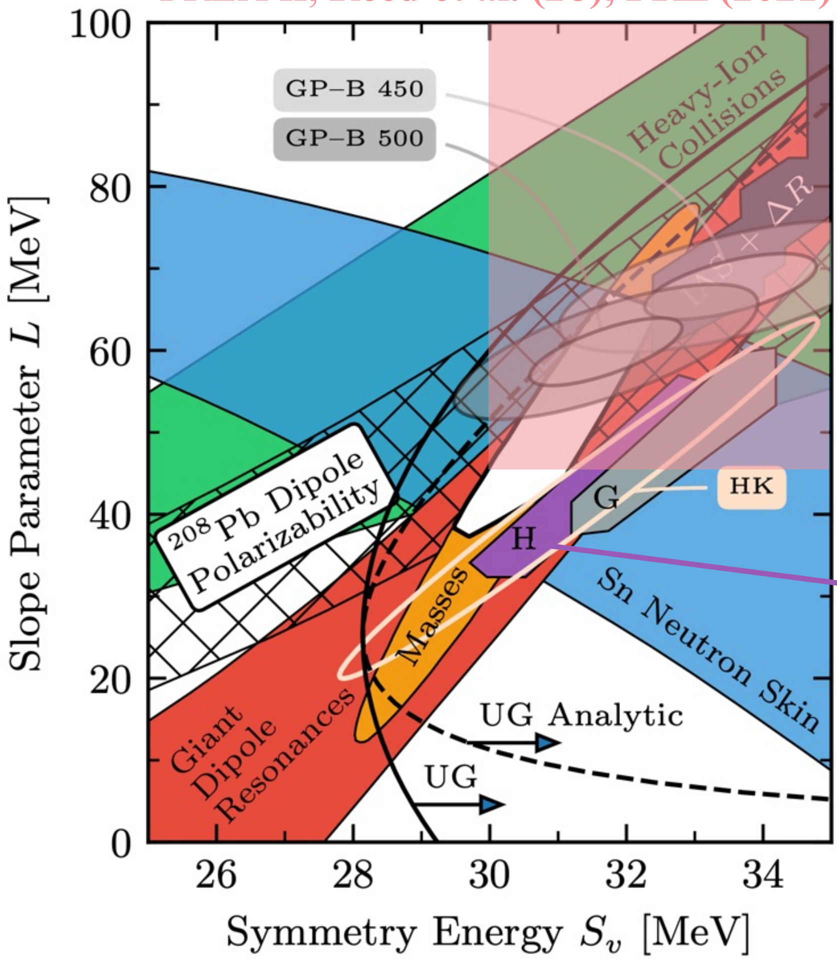

Ab initio calc of ^{208}Pb neutron skin

Hu, Jiang, Miyagi et al., arXiv:2112.01125

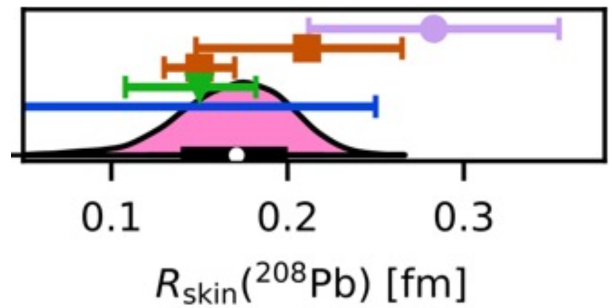

Region H corresponds to ^{208}Pb neutron skin: 0.14-0.20 fm

Hebeler, Lattimer, Pethick, AS, PRL (2010)

from Drischler, Holt, Wellenhofer, AS, ARNPS (2021)

Note: not all regions are at same saturation density

Impact of PREX and ^{208}Pb dipole polarizability

Essick, Landry, AS, Tews, PRL, PRC (2021)

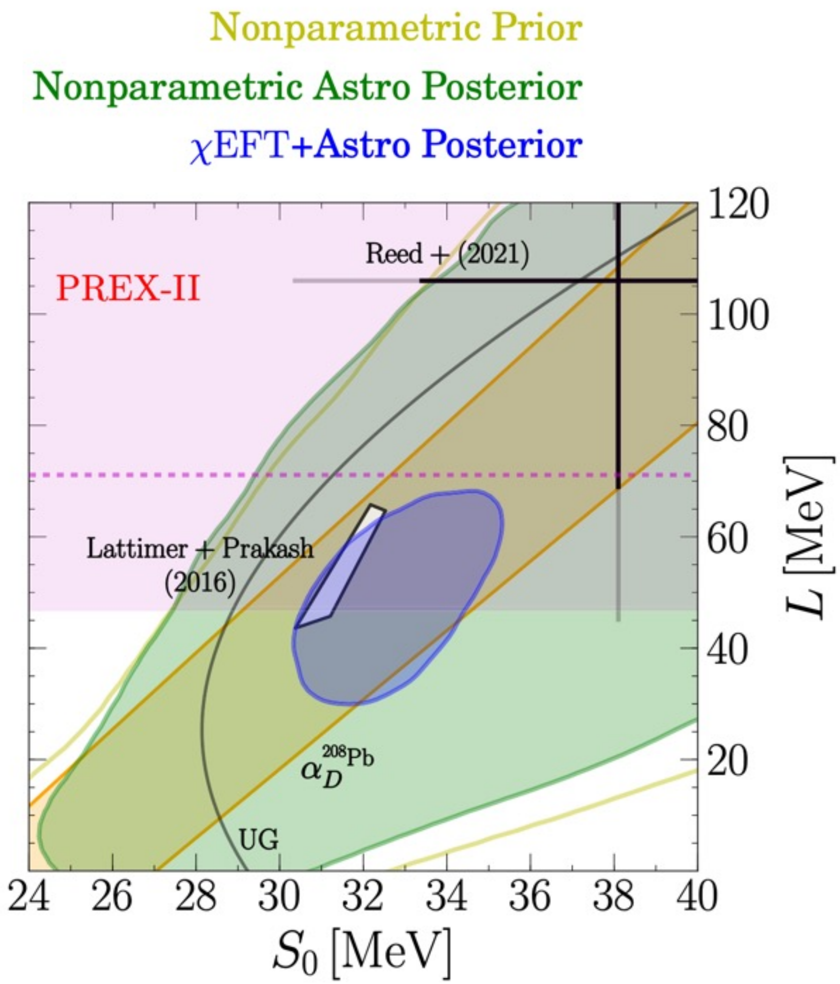

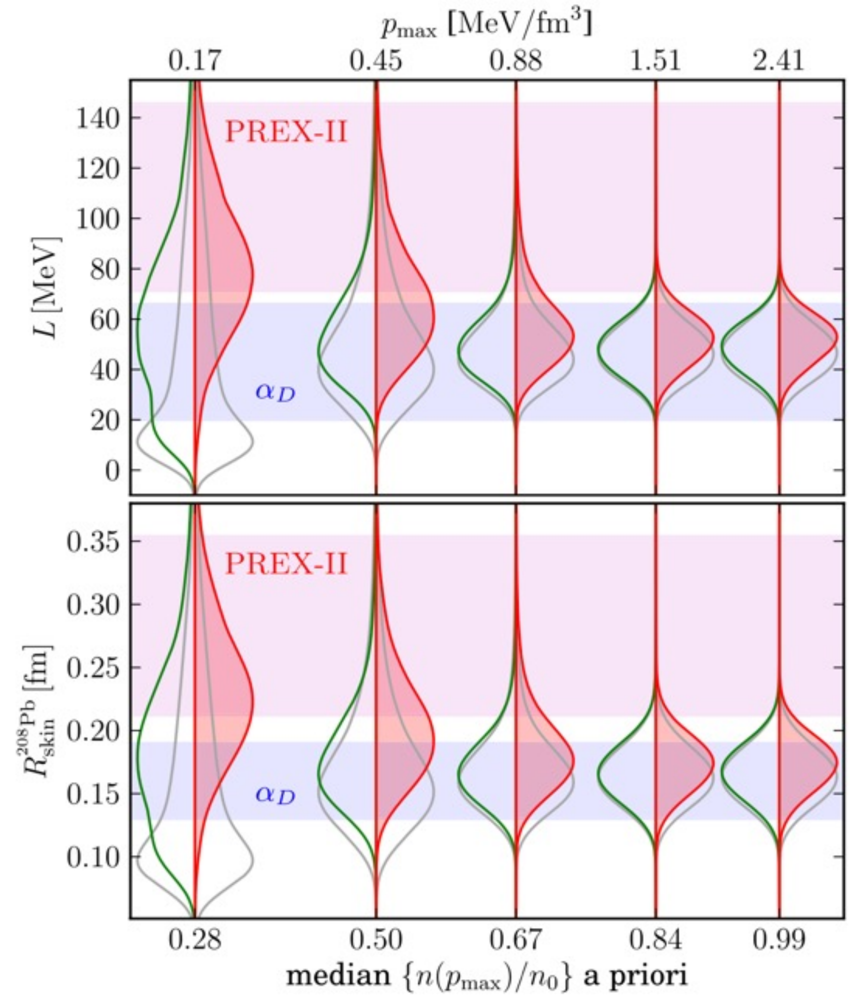

FIG. 2. Prior (gray, unshaded), Astro posterior (green, left-unshaded), and Astro + PREX-II posterior (red, right-shaded)

^{208}Pb dipole polarizability Tamii et al., PRL (2021)

very consistent with χEFT+Astro posterior

Neutron skin and dipole polarizability of ^{48}Ca

Hagen et al., Nature Phys. (2015)

ab initio calculations lead to charge distributions consistent with exp,

predict **small neutron skin** **dipole polarizability α_D**

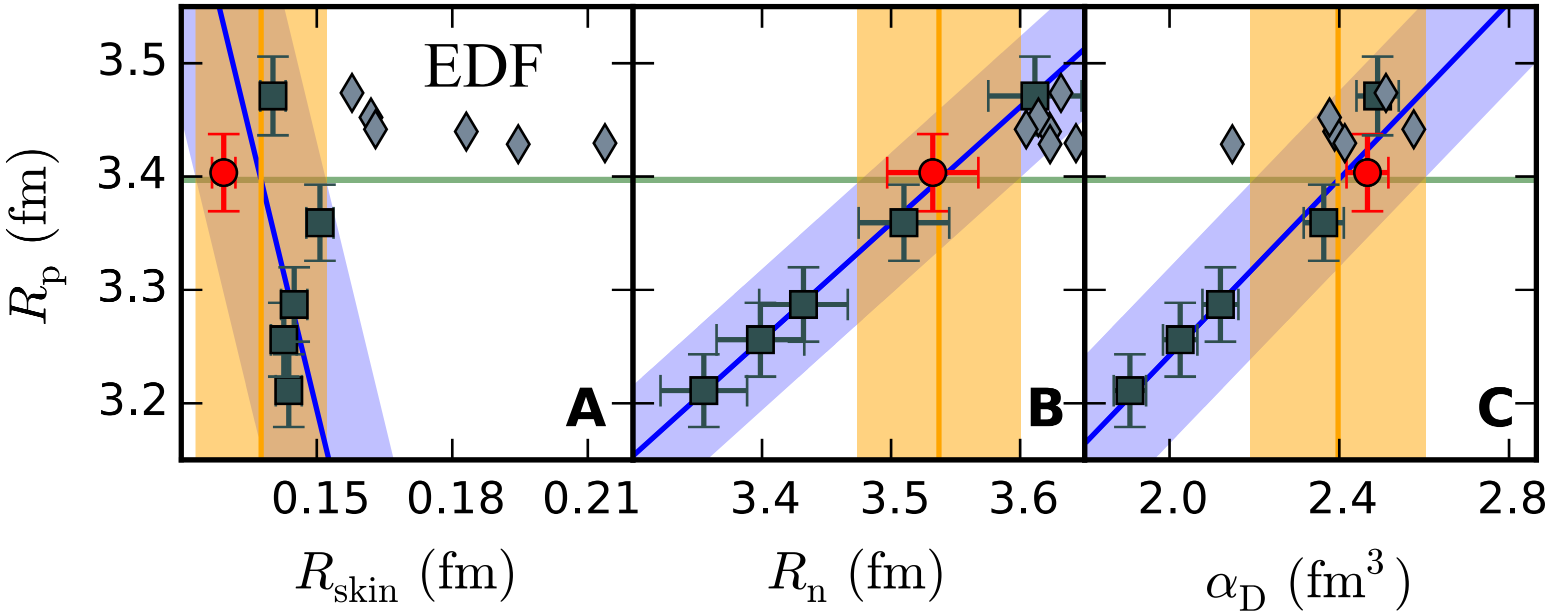

Neutron skin and dipole polarizability of ^{48}Ca

Hagen et al., Nature Phys. (2015)

ab initio calculations lead to charge distributions consistent with exp,

predict **small neutron skin** **dipole polarizability α_D**

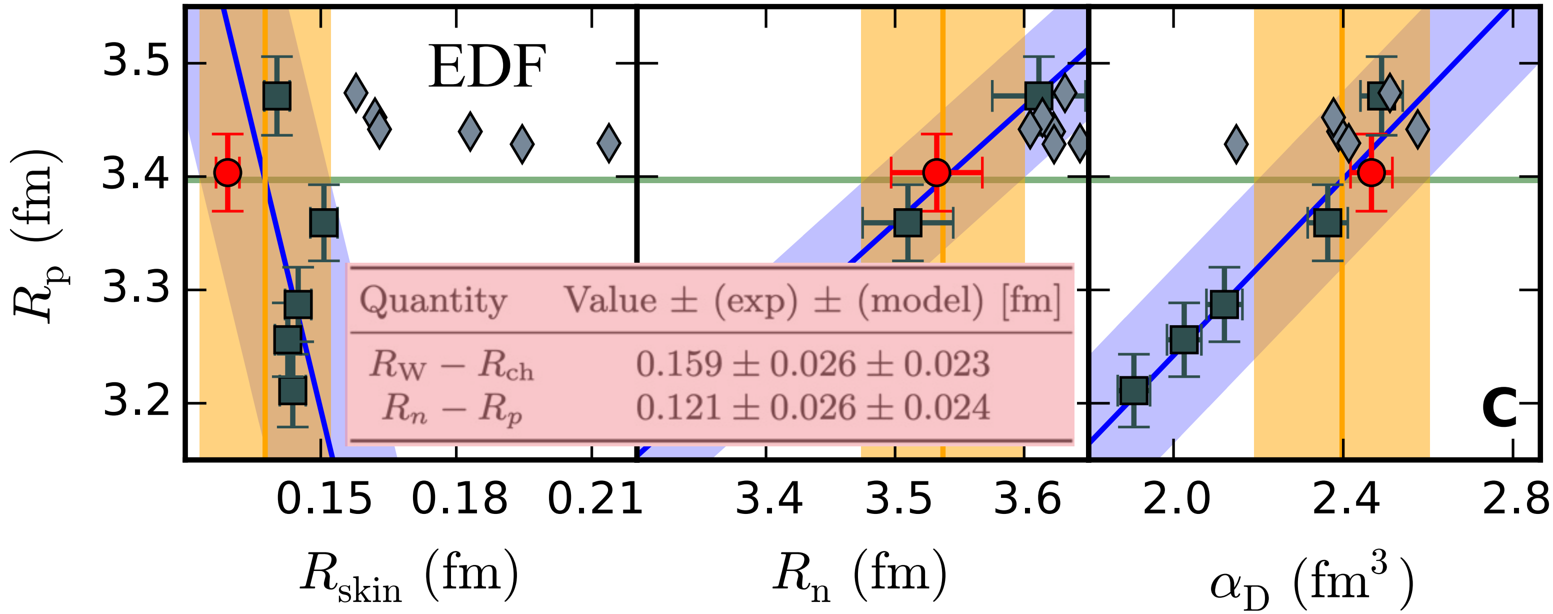

agrees with dipole polarizability from Darmstadt-Osaka exp Birkhan et al., PRL (2017)

+ with CREX result Adhikari et al., PRL (2022)